

FEEDBACK SYSTEM MODELING AND DESIGN TOOLS

This chapter uses techniques developed previously, especially those in Section 13.5, to consider some of the problems encountered in modeling and designing feedback control systems. In order to introduce the reader to some of the typical concerns, we first examine in detail a particular electromechanical system. We construct a block-diagram model, find the transfer function, and then improve the performance by adjusting those parameters that are under the designer's control.

Two important graphical design aids are described in Sections 14.2 and 14.3. The first of these shows how the poles of the transfer function move when one of the system parameters is varied. The second represents the sinusoidal steady-state response by diagrams that are convenient for system design.

In the final two sections we explain and illustrate some of the practical design criteria and ways of meeting those criteria. We include stability considerations, the transient response, the steady-state errors corresponding to particular inputs, the need for satisfactory performance even if the system parameters change somewhat, minimizing the response to unwanted disturbance inputs, and rejecting unwanted noise.

■ 14.1 APPLICATION TO A CONTROL SYSTEM

Most control systems use feedback to force the output variable to follow a reference input while remaining relatively insensitive to the effects of one or more disturbance inputs. A common type of control system is the **servomechanism**. Here a mechanical input variable, such as the position

or angular rotation of an element, is required to follow a reference input, such as the orientation of a knob or dial that is varied by a human operator. For example, a mechanical manipulator used for working with radioactive materials would require several servomechanisms to translate the operator's hand motion into equivalent physical motion at a remote location behind the shielding material.

In this section, we model and analyze a simple servomechanism whose purpose is to make the angular orientation of an output shaft follow that of a manually adjusted dial. First, we will develop a mathematical model of the feedback system by writing the algebraic and differential equations that describe the individual elements, transforming these equations and drawing a block diagram, and then reducing the block diagram to give a single transfer function. Finally, we shall analyze the system's performance and consider means of improving it.

System Description

The positional servomechanism we will consider is shown in Figure 14.1. The manually set input potentiometer at the left has its two ends connected to constant voltage sources, and its wiper voltage e_1 obeys the algebraic relationship

$$e_1 = K_\theta \theta_i(t) \quad (1)$$

where K_θ is a constant, provided that the potentiometer is linear and that no current is drawn by the amplifier—that is, there is no loading. The output potentiometer at the right of the figure is identical to the input potentiometer, except that its wiper is mechanically connected to the output shaft. Hence the voltage of the wiper of the output potentiometer obeys the equation

$$e_2 = K_\theta \theta_o \quad (2)$$

If both potentiometers are constrained to one full revolution and if the constant voltage sources are $\pm A$ volts, then $K_\theta = A/\pi$ volts per radian.

The amplifier's output voltage is

$$e_a = K_A(e_1 - e_2) \quad (3)$$

where K_A is the amplifier gain in volts per volt. It is assumed that (3) holds regardless of the current i flowing in the armature circuit of the motor and that the amplifier draws no current from the wipers of the input and output potentiometers. Note that the amplifier is described by an algebraic rather than a differential equation, which implies that (3) holds regardless of how rapidly e_1 or e_2 may vary.

The motor is assumed to have a constant field current and negligible inductance in the armature winding. The electromechanical driving torque τ_e and the induced voltage e_m are given, as in (10.29), by

$$\tau_e = \alpha i$$

$$e_m = \alpha \dot{\phi}$$

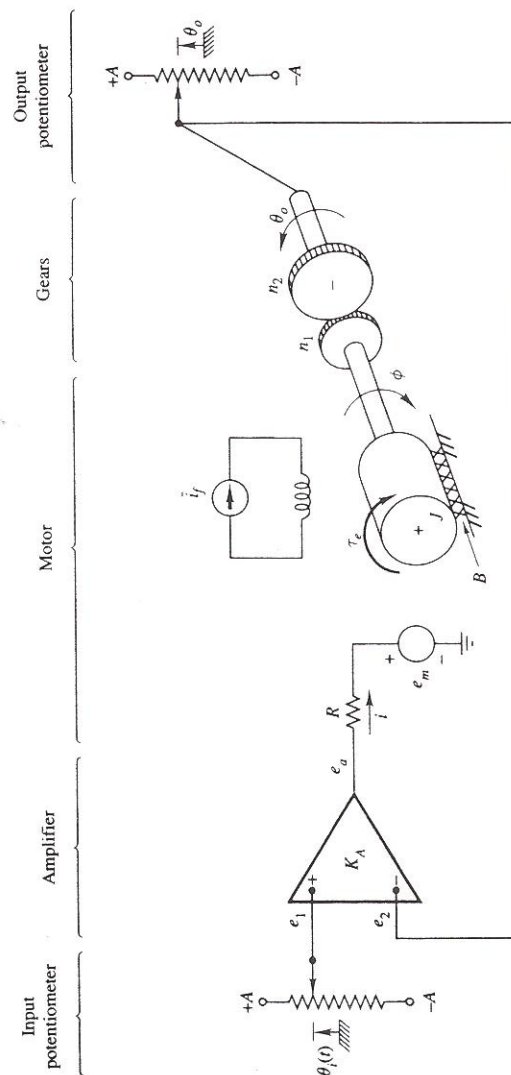


FIGURE 14.1 Servomechanism components.

where the coupling coefficient α has units of volt-seconds or, equivalently, newton-meters per ampere and is dependent on the field current i_f . The symbol ϕ denotes the angular displacement of the motor shaft. If the armature resistance is denoted by R , the viscous-friction coefficient by B , and the moment of inertia by J , the motor can be modeled by the pair of equations

$$i = \frac{1}{R}(e_a - \alpha\dot{\phi}) \quad (4a)$$

$$J\ddot{\phi} + B\dot{\phi} = \alpha i \quad (4b)$$

The motor shaft is connected to the output shaft through a pair of gears having the gear ratio $N = n_2/n_1$. Hence the motor angle ϕ and the output wiper angle θ_o are related by

$$\theta_o = \frac{1}{N}\phi \quad (5)$$

Although Figure 14.1 does not indicate a moment of inertia attached to the right gear or moments of inertia for the gears themselves, such moments of inertia could be referred to the motor shaft and incorporated in the value of J if they were not negligible. Likewise, any viscous friction associated with the output shaft could be referred to the motor and combined with B .

System Model

In order to obtain a block diagram for the system, we transform (1) through (5) with zero initial conditions. For the combination of the input and output potentiometers and the amplifier, substituting (1) and (2) into (3) and taking the Laplace transform yield

$$E_a(s) = K_A K_\theta [\Theta_i(s) - \Theta_o(s)] \quad (6)$$

which is represented by the two gains of K_θ , the summing junction, and the gain of K_A within the dashed rectangle shown in Figure 14.2.

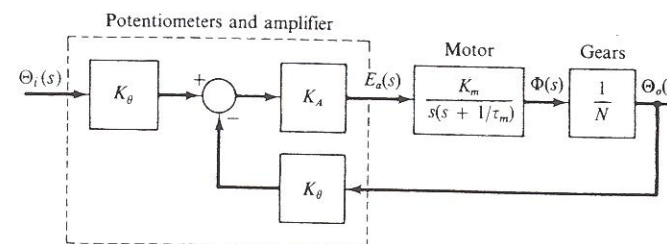


FIGURE 14.2 Servomechanism block diagram.

When (4) is transformed and $I(s)$ is eliminated, we obtain the single transformed equation

$$\left[Js^2 + \left(B + \frac{\alpha^2}{R} \right) s \right] \Phi(s) = \frac{\alpha}{R} E_a(s)$$

for the motor, which yields the transfer function

$$\frac{\Phi(s)}{E_a(s)} = \frac{\frac{\alpha}{RJ}}{s \left[s + \left(\frac{B}{J} + \frac{\alpha^2}{JR} \right) \right]}$$

If we define the parameters

$$K_m = \frac{\alpha}{RJ}$$

$$\tau_m = \frac{1}{\frac{B}{J} + \frac{\alpha^2}{JR}}$$

the transfer function of the motor becomes

$$\frac{\Phi(s)}{E_a(s)} = \frac{K_m}{s \left(s + \frac{1}{\tau_m} \right)} \quad (7)$$

which results in a single block located in the forward path of the diagram shown in Figure 14.2. Finally, we describe the gears by the gain $1/N$ according to

$$\Theta_o(s) = \frac{1}{N} \Phi(s) \quad (8)$$

and draw the feedback path from the output to the output-potentiometer block.

Closed-Loop Transfer Function

To calculate $T(s) = \Theta_o(s)/\Theta_i(s)$, the transfer function of the closed-loop system, we note that the first block with gain K_θ is in series with the feedback-loop portion of the system. We can obtain the transfer function of the feedback loop by applying (13.46) with

$$G(s) = \frac{K_A K_m / N}{s(s + 1/\tau_m)}$$

$$H(s) = K_\theta$$

Then

$$T(s) = K_\theta \left[\frac{G(s)}{1 + G(s)H(s)} \right] = \frac{K_A K_m K_\theta / N}{s^2 + (1/\tau_m)s + K_A K_m K_\theta / N} \quad (9)$$

By inspection of (9), we can observe several important aspects of the behavior of the closed-loop system. First, the system model is second-order, and its closed-loop transfer function $T(s)$ has two poles and no zeros in the finite s -plane. Assuming that the values of all the parameters appearing in $T(s)$ are positive, the poles of $T(s)$ will be in the left half of the complex plane, and the closed-loop system will be stable regardless of the specific numerical values of the parameters.

We obtain the steady-state value of the unit step response of the closed-loop system by setting s equal to zero in (9).

$$T(0) = \frac{K_A K_m K_\theta / N}{K_A K_m K_\theta / N} = 1$$

Hence a step input for $\theta_i(t)$ will result in an output angle θ_o that is identical to the input angle in the steady state. This steady-state condition of zero error will occur regardless of the specific numerical values for the system parameters. This property is a result of the feedback structure of the servomechanism, whereby a signal that is proportional to the error signal $\theta_i(t) - \theta_o$ is used to drive the motor. Because the motor acts like an integrator (its transfer function $\Phi(s)/E_a(s)$ has a pole at $s = 0$), the armature voltage e_a must become zero if the system is to reach steady state with a constant input; otherwise, $\dot{\phi}$ would not be zero. Because of (3), the difference of the wiper voltages e_1 and e_2 must be zero in the steady state, and this condition requires that $(\theta_o)_{ss} = \theta_i$.

Design for Specified Damping Ratio

In practice, all the parameter values except one are often fixed and we must select the remaining one to yield some specific response characteristic such as the damping ratio, undamped natural frequency, or steady-state response. Suppose that all the parameters except the amplifier gain K_A are fixed at the values listed in Table 14.1 and that we must select K_A to yield a value of 0.50 for the damping ratio.

TABLE 14.1 Numerical Values of Servomechanism Parameters

Parameter	Value
A (magnitude of potentiometer voltages)	15.0 V
K_m (for the motor)	150. V · rad/s ²
τ_m (for the motor)	0.40 s
N (gear ratio)	10.

Because the potentiometer gains are $K_\theta = A/\pi$, it follows that $K_\theta = 15.0/\pi = 4.775$ V/rad. Substituting the known parameter values into (9) results in the closed-loop transfer function

$$\begin{aligned} T(s) &= \frac{(15 \times 4.775/10)K_A}{s^2 + (1/0.40)s + (15 \times 4.775/10)K_A} \\ &= \frac{71.62K_A}{s^2 + 2.50s + 71.62K_A} \end{aligned} \quad (10)$$

Comparing the denominator of (10) to the polynomial $s^2 + 2\xi\omega_n s + \omega_n^2$, which is used to define the damping ratio ξ and the undamped natural frequency ω_n , we see that

$$2\xi\omega_n = 2.50 \quad (11a)$$

$$\omega_n^2 = 71.62K_A \quad (11b)$$

Setting ξ equal to its specified value of 0.50 in (11a), we get $\omega_n = 2.50$ rad/s. Substituting for ω_n^2 in (11b) gives the required amplifier gain as

$$K_A = 0.08727 \text{ V/V}$$

Substituting this value of K_A into (10) yields the closed-loop transfer function in numerical form as

$$T(s) = \frac{6.25}{s^2 + 2.50s + 6.25} \quad (12)$$

You can verify that the denominator of $T(s)$ results in a pair of complex poles having $\xi = 0.50$ as specified.

Proportional-Plus-Derivative Feedback

The system designed in the foregoing paragraphs is constrained in several ways that turn out to be undesirable in practice. For example, although we obtained the specified damping ratio of 0.50, the value of ω_n was dictated by the requirement on ξ and could not have been specified independently. In practice, one might want to specify both ξ and ω_n for the closed-loop system. We shall demonstrate that this can be done, provided that a signal proportional to the angular velocity of the motor shaft (or output shaft) is fed back and added to the amplifier input.

Assume that a tachometer is attached directly to the motor and a potentiometer is placed across the output terminals of the tachometer, such that the voltage on the potentiometer wiper is

$$e_3 = K_T \dot{\phi}$$

where K_T has units of volt-seconds and is adjustable between zero and some positive maximum value. The signal e_3 is added to e_2 , such that the armature voltage is now

$$\begin{aligned} e_a &= K_A(e_1 - e_2 - e_3) \\ &= K_A[K_\theta\theta_i(t) - K_\theta\theta_o - K_T\dot{\phi}] \end{aligned}$$

Then the transform of the armature voltage becomes

$$E_a(s) = K_A[K_\theta\Theta_i(s) - K_\theta\Theta_o(s) - K_Ts\Phi(s)] \quad (13)$$

The modified system can be represented by the block diagram shown in Figure 14.3, which we obtain by separating the motor transfer function $K_m/[s(s+1/\tau_m)]$ into the pair of blocks in series shown in the figure and then adding the inner feedback path corresponding to the term $K_Ts\Phi(s)$. Because we assume zero initial conditions when evaluating transfer functions, the input to the gain block K_T is $s\Phi(s) = \mathcal{L}[\dot{\phi}(t)]$. Thus a signal proportional to the angular velocity of the motor shaft is being fed through the inner feedback path to the summing junction.

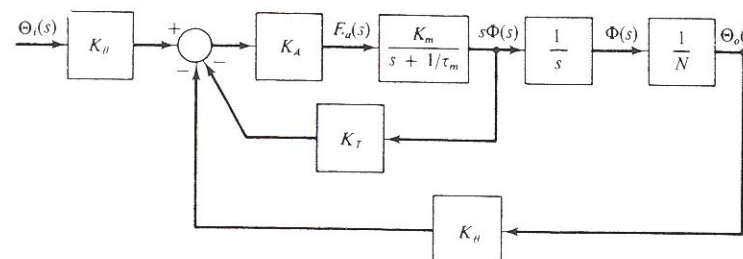


FIGURE 14.3 Block diagram of servomechanism with tachometer feedback added.

To determine the effect of the tachometer feedback on the closed-loop transfer function, we can reduce the inner loop shown in Figure 14.3 by using (13.46) with $G(s) = K_A K_m / (s + 1/\tau_m)$ and $H(s) = K_T$ to give

$$T'(s) = \frac{K_A K_m}{s + (1/\tau_m) + K_A K_m K_T}$$

Applying (13.46) again with $G(s) = T'(s)/sN$ and $H(s) = K_\theta$ and then multiplying the result by K_θ , we obtain the overall transfer function

$$T(s) = \frac{K_A K_m K_\theta / N}{s^2 + [(1/\tau_m) + K_A K_m K_T]s + K_A K_m K_\theta / N} \quad (14)$$

Comparing (14) to (9) indicates that the only effect of the tachometer feedback is to modify the coefficient of s in the denominator of the transfer function. Hence the damping ratio and undamped natural frequency now satisfy the relationships

$$\begin{aligned} 2\zeta\omega_n &= (1/\tau_m) + K_A K_m K_T \\ \omega_n^2 &= K_A K_m K_\theta / N \end{aligned} \quad (15)$$

If the values of both K_A and K_T can be selected with τ_m , K_m , K_θ , and N fixed as before, we can specify values for both ζ and ω_n . For example, using the parameter values given in Table 14.1 with $\zeta = 0.50$, we find that (15) reduces to

$$\omega_n = 2.50 + 150K_A K_T \quad (16a)$$

$$\omega_n^2 = 71.62K_A \quad (16b)$$

If, for example, we want ω_n to be 5.0 rad/s, it follows that

$$K_A = 0.3491 \text{ V/V}$$

$$K_T = 0.04775 \text{ V}\cdot\text{s/rad}$$

When we substitute these parameter values and those listed in Table 14.1 into (14), the numerical form of the closed-loop transfer function with tachometer feedback is

$$T(s) = \frac{25.0}{s^2 + 5.0s + 25.0}$$

It is easy to verify that the two poles of $T(s)$ are complex and have $\zeta = 0.50$ and $\omega_n = 5.0 \text{ rad/s}$, as required.

In concluding this example, we note that the control law given by (13) uses a combination of the output-shaft angle θ_o and the motor angular velocity $\dot{\phi}$ as the feedback signals. It is also possible to think in terms of having the output-shaft angular velocity $\dot{\theta}_o$ fed back by noting that the two angular velocities in question are proportional to one another: $\dot{\theta}_o = \dot{\phi}/N$. Hence we can rewrite (13) in the time domain and in terms of the output-shaft angle as

$$e_a = K_A [K_\theta \theta_i(t) - K_\theta \theta_o - K_\theta \dot{\theta}_o] \quad (17)$$

where $K_\theta = NK_T$, which is the gain of the angular-velocity term. The block diagram corresponding to this version of the control law can take either of the equivalent forms shown in Figure 14.4. If we combine the two parallel feedback paths shown in Figure 14.4(b) to yield the single feedback transfer function $K_\theta + K_\theta s$, using (13.46) gives the same expression for $T(s) = \Theta_o(s)/\Theta_i(s)$ as found in (14).

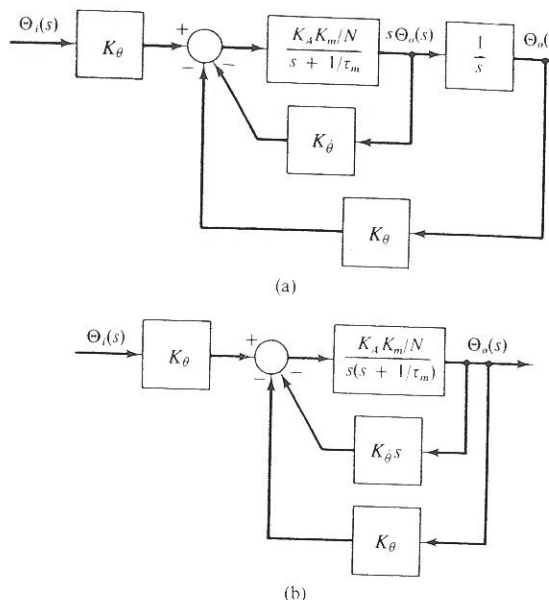


FIGURE 14.4 Equivalent block diagrams for servomechanism with tachometer feedback.

■ 14.2 ROOT-LOCUS DIAGRAMS

The poles of a system's overall transfer function determine whether the system is stable and, for a stable system, determine the nature of the transient response. Because the positions of the poles in the complex s -plane constitute one of the key design considerations, it is important to know how these positions change when one of the parameters of the system is varied.

The effect of the pole positions on stability and on the transient response was discussed in detail in Chapters 6 and 8. Keep in mind that the poles of the transfer function are roots of the characteristic polynomial used in Chapter 6. If all the poles are inside the left half of the s -plane, then the free response decays to zero and the system is stable. If the transfer function has a pole inside the right half-plane or repeated poles on the imaginary axis, the free response increases without limit and the system is unstable. Finally, if all the poles are inside the left half-plane except for first-order poles on the imaginary axis (possibly including the origin), a nonzero but finite component of the free response remains for large values of t , and the system is said to be marginally stable.

The nature of the free response corresponding to various pole positions was illustrated in Figures 6.17 through 6.20. For a single pole on the negative

real axis of the s -plane, the distance from the vertical axis is the reciprocal of the time constant. For a pair of first-order poles at $s = -\alpha \pm j\beta$ in the left half-plane, the free response has the form

$$y_H(t) = K e^{-\alpha t} \cos(\beta t + \phi)$$

where α , the distance from the vertical axis, is again the reciprocal of the time constant for the exponential factor.

The movement of the pole positions when a particular parameter is varied can be shown by drawing the path traced out in the s -plane as the parameter is increased from very small to very large values. Because poles of the transfer function are roots of the characteristic equation, such a path is called a **root locus**. It can help us select appropriate values for some of the elements. Although we shall not use it in this way, it can also help us determine how sensitive the pole positions are to unwanted variations in the system components.

Most root-locus diagrams are drawn for the closed-loop transfer function of a standard feedback configuration, and this will be our primary interest. However, we shall first illustrate the concept of a locus of possible pole positions by examining two mechanical systems that do not have external feedback paths.

► EXAMPLE 14.1

For the first-order system shown in Figure 14.5(a), find the locus traced out by the pole of $T(s) = V(s)/F_a(s)$ when the friction coefficient B is varied from zero to infinity.

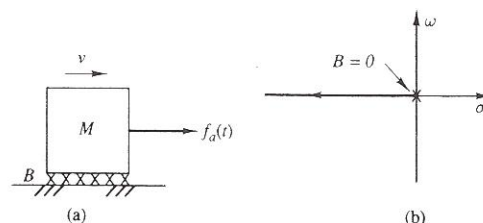


FIGURE 14.5 (a) Mechanical system for Example 14.1.
(b) Locus of pole positions when B is varied.

Solution

The differential equation describing the system is $M\ddot{v} + Bv = f_a(t)$, so the transfer function is

$$T(s) = \frac{1}{Ms + B}$$

14.2 Root-Locus Diagrams

which has a single pole at $s = -B/M$. When $B = 0$, the pole is at the origin of the s -plane and is shown by the cross in Figure 14.5(b). The free response will not decay to zero for this case, because there is no retarding frictional force.

As B increases, the pole moves to the left, as indicated by the arrow in the figure. As expected, we see that the free response decays more and more quickly as B is increased.

Finding the locus for each part of the next example is more complicated, but the general procedure is the same. At the end of this section, we shall show how to put the transfer function into a form that enables us to use some special techniques to obtain the locus more easily.

► EXAMPLE 14.2

Consider the transfer function $T(s) = X(s)/F_a(s)$ for the second-order mechanical system shown in Figure 14.6(a). First assume that M and B have fixed values. Find the locus traced out by the poles of $T(s)$ as the spring constant K is increased from zero toward infinity. Repeat the problem when M and K are fixed, while the friction coefficient B is varied from zero toward infinity.

Solution

The input-output differential equation is easily shown to be $M\ddot{x} + B\dot{x} + Kx = f_a(t)$, so the transfer function is

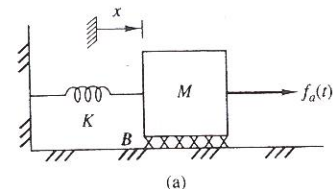
$$T(s) = \frac{1}{Ms^2 + Bs + K} = \frac{\frac{1}{M}}{s^2 + \frac{B}{M}s + \frac{K}{M}}$$

Because the denominator of $T(s)$ is a quadratic, there are two poles. When $K = 0$, these poles are at $s = 0$ and $s = -B/M$, as indicated by the crosses in Figure 14.6(b). When $K = B^2/4M$, the denominator becomes

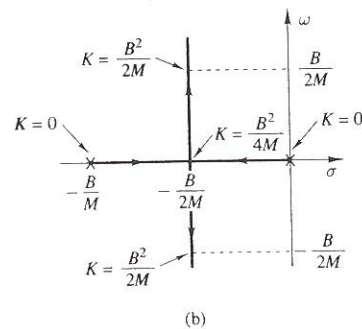
$$s^2 + \frac{B}{M}s + \frac{B^2}{4M^2} = \left(s + \frac{B}{2M}\right)^2$$

For this value of K , there is a double pole at $s = -B/2M$. For values of K larger than $B^2/4M$, it is convenient to rewrite the denominator of the transfer function by completing the square (Section 7.3):

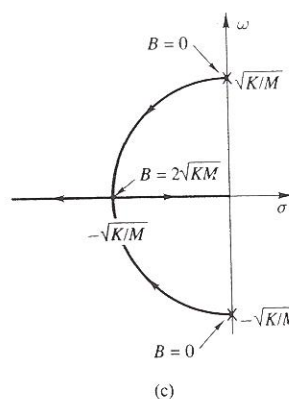
$$T(s) = \frac{\frac{1}{M}}{\left(s + \frac{B}{2M}\right)^2 + \left(\frac{K}{M} - \frac{B^2}{4M^2}\right)}$$



(a)



(b)



(c)

FIGURE 14.6 (a) Mechanical system for Example 14.2. (b) Locus of pole positions when K is varied. (c) Locus of pole positions when B is varied.

which has poles at

$$s = -\frac{B}{2M} \pm j\sqrt{\frac{K}{M} - \frac{B^2}{4M^2}} = \frac{1}{2M} \left[-B \pm j\sqrt{4KM - B^2} \right] \quad (18)$$

For constant values of M and B , the real part of this expression is constant, whereas the size of the imaginary part increases as K increases. The heavy

lines in Figure 14.6(b) constitute the complete locus of all possible pole positions for nonnegative values of K . The arrows on the locus indicate the directions in which the poles move as K is increased. The values of K corresponding to some of the specific points are also shown.

For the case where M and K are fixed, we first let $B = 0$. The poles of $T(s)$ are then at $s = \pm j\sqrt{K/M}$, as indicated by the crosses in Figure 14.6(c). For $0 < B < 2\sqrt{KM}$, we have a pair of complex conjugate poles in the left half-plane, as given by (18). The distance of these poles from the origin of the s -plane is

$$\frac{1}{2M} [B^2 + (4KM - B^2)]^{1/2} = \sqrt{K/M}$$

Thus for constant values of K and M , this part of the locus is the arc of a circle of radius $\sqrt{K/M}$. When $B = 2\sqrt{KM}$, the denominator of $T(s)$ becomes

$$M(s^2 + 2\sqrt{K/M}s + K/M) = M(s + \sqrt{K/M})^2$$

corresponding to a double pole on the negative real axis at $s = -\sqrt{K/M}$. For values of B larger than $2\sqrt{KM}$, there are two distinct poles on the negative real axis. The complete locus traced out by the pole positions is shown by the heavy lines. The arrows indicate increasing values of B .

Although a locus of possible pole positions can be drawn for any system in which only one of the parameters is varied, it is particularly important for us to be able to do this for the feedback configuration shown in Figure 13.22(a), which is repeated in Figure 14.7. From (13.46), the closed-loop transfer function is

$$T(s) = \frac{G(s)}{1 + G(s)H(s)} \quad (19)$$

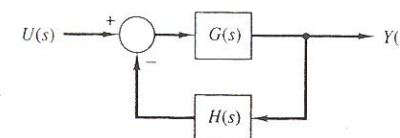


FIGURE 14.7 Block diagram of a feedback system.

We shall assume that the open-loop transfer function $G(s)H(s)$ can be expressed in factored form as

$$G(s)H(s) = K \frac{(s - z_1) \cdots (s - z_m)}{(s - p_1) \cdots (s - p_n)} \quad (20a)$$

$$= K F(s) \quad (20b)$$

Note from this definition that $F(s)$ contains all the factors of $G(s)H(s)$ except the multiplying constant K . Parts of $G(s)H(s)$ are normally under the control of the designer, who typically takes a particular $F(s)$ and then sketches a locus of the poles of $T(s)$ as K is varied. The designer can do this *without* having first to write $T(s)$ as an explicit rational function and without having to factor high-order polynomials.

The quantities z_1 through z_m in (20) are the zeros of $F(s)$ in the finite s -plane, which are referred to as the **open-loop zeros**. The quantities p_1 through p_n are the poles, referred to as the **open-loop poles**. For all practical physical systems $m \leq n$. If $m < n$, then $F(s)$ is said to have a zero of order $n - m$ at infinity. We seek a locus of the poles of $T(s)$ as the positive constant K is varied. The poles of the closed-loop transfer function $T(s)$ will lie on the root locus and will be called roots. In the ensuing discussion, the terms *poles* and *zeros* refer to p_i and z_j , respectively, in the open-loop transfer function $KF(s)$.

Chapter 15 will describe a computer program that can be used to construct the root locus when $F(s)$ is given. However, it is helpful to be able to predict the general shape of the locus, even if one plans to rely on a computer program for an exact final plot. Books on feedback control systems, including several of the references in Appendix D, develop a number of rules for sketching the locus by hand. We shall present here, without proof, the most useful of these rules.

Angle and Magnitude Criteria

We see from (19) that the poles of $T(s)$, which are the points on the root locus, will be those values of s for which

$$1 + G(s)H(s) = 0$$

With $G(s)H(s)$ replaced by $KF(s)$, this requires that $1 + KF(s) = 0$, so

$$KF(s) = -1 \quad (21)$$

The quantity on the right-hand side of (21) has a magnitude of 1 and an angle of π radians (or any odd multiple of π radians). Thus if the constant K is restricted to positive values, the angle criterion is

$$\arg F(s) = \pm n\pi \text{ for } n = 1, 3, 5, \dots \quad (22)$$

and the magnitude criterion is

$$K = \frac{1}{|F(s)|} \quad (23)$$

We use (22), which does not involve K , to find the locus of *all possible* root positions for $K \geq 0$. Then we can use (23) to calibrate the locus—that is, to find the values of K that correspond to particular points on the locus.

Rules for Constructing a Root Locus

Some of the rules may seem intuitively obvious. For example, because any complex poles must occur in conjugate pairs, the root locus must be symmetrical about the real axis. Root locations must satisfy (23), so K must be small for points on the locus close to the poles of $F(s)$. Similarly, K must be large for points close to the zeros of $F(s)$. Other rules are much less obvious, but they are summarized below for the case where $K \geq 0$ and where the poles and zeros are distinct. We let n denote the number of poles of $F(s)$, and m the number of finite-plane zeros. After presenting the rules, we shall illustrate them with several examples.

1. The locus is symmetrical with respect to the real axis of the s -plane.
2. The locus has n branches.
3. A point on the real axis is part of the locus if and only if the total number of real poles and zeros to the right of that point is odd.
4. If a single pair of branches in the locus leaves or enters the real axis, those branches do so at angles of ± 90 degrees.
5. As K increases from zero, one branch of the locus departs from each of the poles of $F(s)$.
6. As K approaches infinity, the branches of the locus approach the zeros of $F(s)$. There will be m branches approaching the finite-plane zeros. If $m \neq n$, the remaining $n - m$ branches will approach infinity.
7. The branches approaching infinity will be asymptotic to equally spaced straight lines emanating from the center of mass for the poles and zeros. This center can be found by regarding each pole as a positive unit mass and each zero as a negative unit mass, and it is a point on the real axis given by

$$\sigma_0 = \frac{1}{n-m} \left[\sum_{k=1}^n p_k - \sum_{i=1}^m z_i \right] \quad (24)$$

The angles of the equally spaced asymptotes can be determined by remembering that the branches of the locus must be symmetrical about the real axis of the s -plane. Figure 14.8 shows these angles when $n - m$, the number of branches approaching infinity, is 4, 3, or 2. In all cases, the poles of $F(s)$ are at $s = -1, -2, -4$, and -7 . The points on the real axis at which the asymptotes meet can be found from (24) and are at $\sigma = -3.5, -3$, and -4 , respectively. Whenever $n - m$ is an odd integer, one of the asymptotes is the negative real axis.

Other rules can also be developed. One of these gives the angles at which the branches depart from a pair of complex poles of $F(s)$ and the

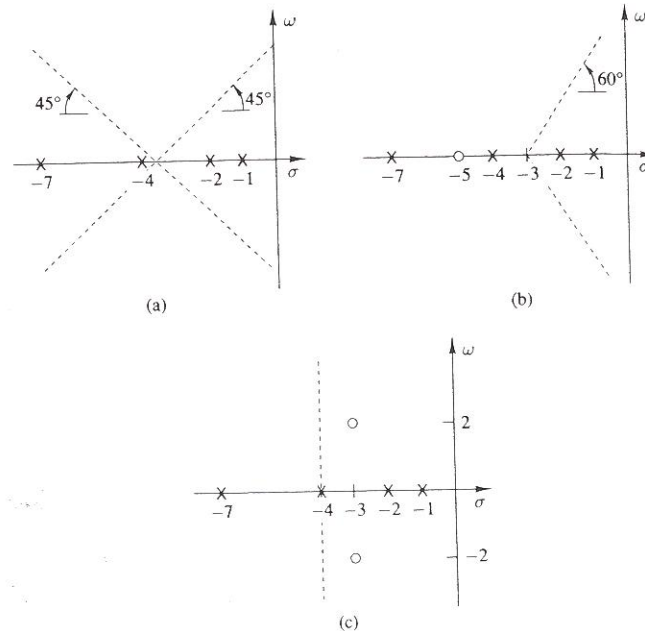


FIGURE 14.8 Asymptotes for branches going to infinity. (a) $n - m = 4$.
(b) $n - m = 3$. (c) $n - m = 2$.

angles at which they approach any complex zeros. However, rather than investigating any other rules, we shall consider a number of examples, which should give some appreciation for the forms of typical loci. The examples will also illustrate the rules already discussed.

When sketching the locus by hand, we first mark the open-loop poles and zeros by crosses and circles, determine which parts of the real axis belong to the locus, and draw the asymptotes for any branches going to infinity. One branch must start from each pole of the open-loop transfer function $KF(s)$ and eventually go either to a finite-plane zero or to infinity. When two branches move toward each other along the real axis and meet, they then leave the axis at angles of ± 90 degrees. We shall not describe the sketching process in great detail, because the locus is normally generated by an appropriate computer package. We used MATLAB¹ for most of the examples in this chapter. The figures are not exact copies of the computer output, but have been modified in order to emphasize the salient features of each plot.

¹MATLAB is described and illustrated in Sections 15.1 and 15.2.

► EXAMPLE 14.3

Find the locus for the poles of the closed-loop transfer function when

$$KF(s) = \frac{K}{s^3 + 7s^2 + 14s + 8} = \frac{K}{(s+1)(s+2)(s+4)}$$

Solution

The parts of the real axis that belong to the locus are indicated by heavy lines. Between $s = -1$ and $s = -2$ there is one pole to the right; for points to the left of $s = -4$ there are three poles to the right (in both cases, an odd integer). Because $F(s)$ has no finite-plane zeros, all three branches of the locus eventually go to infinity. According to (24), the center from which the asymptotes emanate is $\sigma_0 = (-1 - 2 - 4)/3 = -7/3$. The complete plot is shown in Figure 14.9. Arrows indicate the directions in which the closed-loop poles move as K is increased.

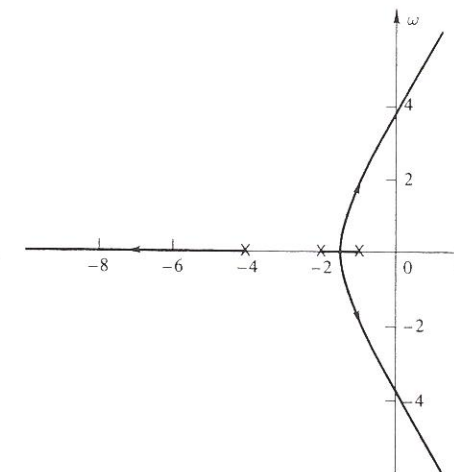


FIGURE 14.9 Root locus for Example 14.3.

Although a root locus shows how the closed-loop poles move as K is increased, it is usually necessary to calibrate the locus by showing the values of K that correspond to specific points. A computer program such as MATLAB can easily list the points on the locus corresponding to specified values of K . If the locus has been sketched by hand, then (23) can be used to evaluate K corresponding to a given point. In the last example, two branches of the locus pass into the right half-plane when K gets sufficiently

large, after which the system becomes unstable. Of particular interest is the value of K for which these two branches are right on the imaginary axis of the s -plane.

► EXAMPLE 14.4

For the function $KF(s)$ in Example 14.3, find the values of the positive constant K for which the closed-loop system is stable.

Solution

We must first determine the height of the two right-hand branches in Figure 14.9 when they are on the imaginary axis. If the locus has been plotted to scale, this can be done by inspection of the figure. For this example, we shall show that the branches cross the axis at $s = \pm j\sqrt{14}$. According to (23), the corresponding value of K is

$$\begin{aligned} K &= \left| \frac{1}{F(s)} \right|_{s=j\sqrt{14}} = |(s+1)(s+2)(s+4)|_{s=j\sqrt{14}} \\ &= |j\sqrt{14} + 1||j\sqrt{14} + 2||j\sqrt{14} + 4| \\ &= \sqrt{15}\sqrt{18}\sqrt{30} = \sqrt{8100} = 90 \end{aligned}$$

For all the branches of the locus to be inside the left half-plane, as is required for a stable system, the positive constant K is restricted to $K < 90$.

The references in Appendix D present special schemes for evaluating the factors in $|F(s)|$ for a particular point in the s -plane. Routh's criterion is useful for finding the value of K that corresponds to a point on the imaginary axis. However, when $F(s)$ has four or fewer poles, the following alternative approach, based on (21), is feasible. In the equation $KF(s) = -1$, we replace s by $j\omega$, corresponding to a point on the imaginary axis a distance ω from the origin. In this example,

$$\frac{K}{-j\omega^3 - 7\omega^2 + j14\omega + 8} = -1$$

Cross-multiplying gives

$$K = (7\omega^2 - 8) + j(\omega^3 - 14\omega)$$

from which we have the pair of equations

$$K = 7\omega^2 - 8 \quad (25a)$$

$$0 = \omega(\omega^2 - 14) \quad (25b)$$

Equation (25b) could be satisfied by $\omega = 0$, but this would correspond to a negative value of K in (25a). Thus we use $\omega = \pm\sqrt{14}$. Substituting this into (25a) gives $K = 98 - 8 = 90$, which agrees with the answer we found before.

► EXAMPLE 14.5

Find the root locus when

$$KF(s) = \frac{K}{(s+1)(s+6-j2)(s+6+j2)}$$

Solution

It is straightforward to find the part of the real axis that belongs to the locus and to draw the asymptotes for the three branches going to infinity. The asymptotes meet at $\sigma_0 = (-1 - 6 + j2 - 6 - j2)/3 = -13/3$. The two branches starting from the complex poles meet at the real axis and then split. One of these branches then meets the branch starting at $s = -1$, after which they eventually move into the right half-plane. The complete locus is shown in Figure 14.10. By the method used in the last example, it can be shown that the overall system is stable when the positive constant K is less than 636.

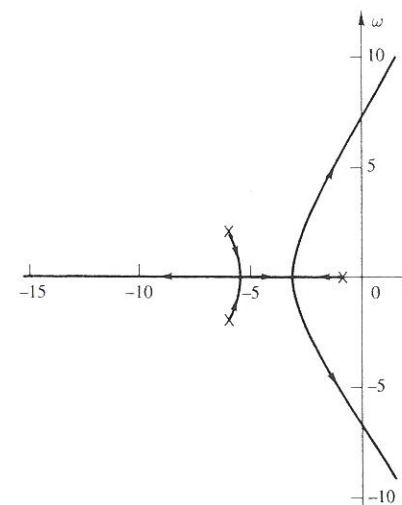


FIGURE 14.10 Root locus for Example 14.5.

► EXAMPLE 14.6

Find the root locus for

$$KF(s) = \frac{K(s+\alpha)}{(s+1)(s+2)(s+10)}$$

when $\alpha = 6$ and when $\alpha = 2.5$.

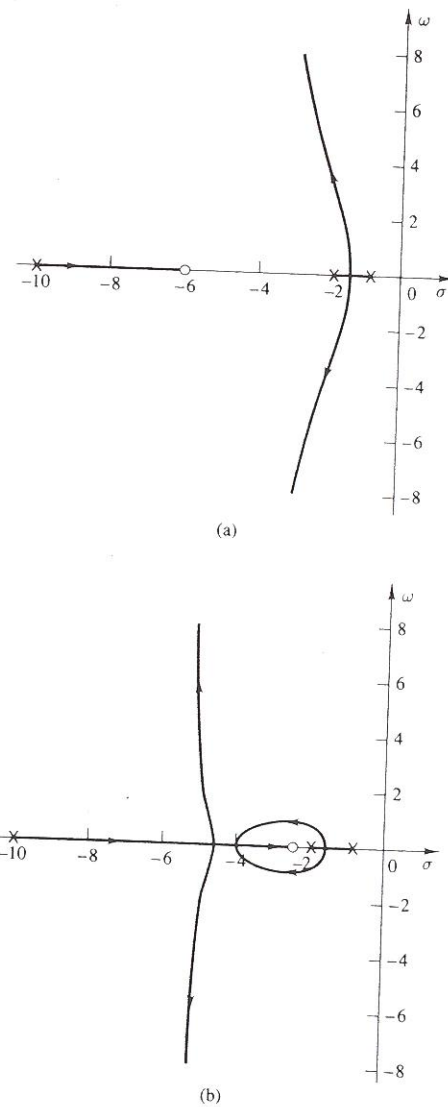


FIGURE 14.11 Root locus for Example 14.6. (a) Zero of $F(s)$ at -6 . (b) Zero of $F(s)$ at -2.5 .

Solution

In both cases, there is one zero of $F(s)$ between the poles at $s = -2$ and $s = -10$. However, the two root-locus plots, as generated by the MATLAB program and as shown in Figure 14.11, are significantly different. When the zero of $F(s)$ is at $s = -6$, the branches starting at $s = -1$ and $s = -2$ are affected in only a relatively minor way by the presence of the other pole-zero combination. When the zero is moved closer to the rightmost branches, it attracts these branches strongly enough to force them to return to the real axis. This is an example of how the shape of the locus can be affected not just by the general nature of the pole-zero pattern for $F(s)$ but also by the specific numerical values used for the poles and zeros.

► EXAMPLE 14.7

Construct the root locus and find the values of the positive constant K for which the overall system is stable when

$$KF(s) = \frac{K(s+2)}{s^4 + 11s^3 + 34s^2 + 24s} = \frac{K(s+2)}{s(s+1)(s+4)(s+6)}$$

Solution

The parts of the real axis that belong to the locus are found in the usual way. The asymptotes for the three branches that go to infinity meet at the point $\sigma_0 = (-1 + 2 - 4 - 6)/3 = -3$. The complete locus is shown in Figure 14.12. For the points where two of the branches cross the imaginary axis, we may set $KF(j\omega) = -1$, getting

$$K(j\omega + 2) = -(\omega^4 - j11\omega^3 - 34\omega^2 + j24\omega)$$

from which

$$2K = -\omega^4 + 34\omega^2 \quad (26a)$$

$$\omega K = \omega(11\omega^2 - 24) \quad (26b)$$

The solutions of (26b) are $\omega = 0$ (corresponding to $K = 0$) and $K = 11\omega^2 - 24$. Substituting this latter expression into (26a) gives

$$22\omega^2 - 48 = -\omega^4 + 34\omega^2$$

or

$$\omega^4 - 12\omega^2 - 48 = 0$$

The only positive value of ω^2 that satisfies this equation is $\omega^2 = 15.17$, for which $K = 142.8$. The system is marginally stable for $K = 0$ and for $K = 142.8$, and it is stable for $0 < K < 142.8$.

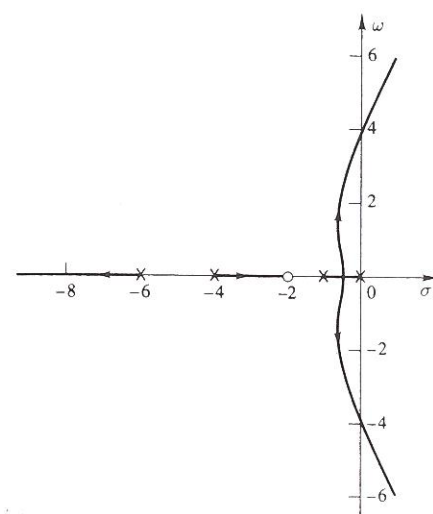


FIGURE 14.12 Root locus for Example 14.7.

► EXAMPLE 14.8

The value of K can be chosen to give a specified damping ratio ζ for a pair of poles in the closed-loop transfer function. Construct the root locus for

$$KF(s) = \frac{K(s^2 + 6s + 10)}{s^2 + 2s + 10} = \frac{K(s + 3 - j1)(s + 3 + j1)}{(s + 1 - j3)(s + 1 + j3)}$$

and determine the range of possible values of ζ when K can be any positive constant.

Solution

The root locus as K is increased from zero to infinity is shown in Figure 14.13. From (6.52), we know that $\zeta = \cos \theta$ for any pair of points on this locus. When $K = 0$, $\zeta = 1/\sqrt{10} = 0.3162$. When K approaches infinity, $\zeta = 3/\sqrt{10} = 0.9487$. By the appropriate choice of K , we can make the damping ratio take on any value between these two limits.

Because this particular example is fairly simple, we can easily find a general expression for ζ in terms of K . Setting $KF(s) = -1$ and cross-multiplying, we have

$$K(s^2 + 6s + 10) = -(s^2 + 2s + 10)$$

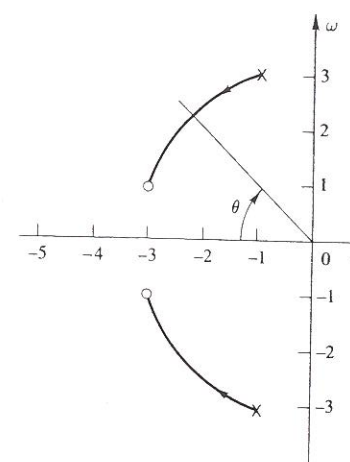


FIGURE 14.13 Root locus for Example 14.8.

Collecting terms and dividing by $K + 1$ give

$$s^2 + \left(\frac{6K + 2}{K + 1} \right) s + 10 = 0$$

This is the closed-loop characteristic equation, whose roots are the poles of the closed-loop transfer function. We can compare this with the standard form of the second-order characteristic equation, $s^2 + 2\xi\omega_n s + \omega_n^2 = 0$, which was first given in (6.50). Then we see that $\omega_n = \sqrt{10}$ and $2\xi\omega_n = (6K + 2)/(K + 1)$, so

$$\xi = \frac{3K + 1}{(K + 1)\sqrt{10}}$$

Replacing K by zero and infinity yields $\xi = 1/\sqrt{10}$ and $\xi = 3/\sqrt{10}$, respectively, which agrees with the previous result. If, for example, we want $\xi = 1/2$, then $(K+1)\sqrt{10} = 2(3K+1)$, from which $\sqrt{10}-2 = (6-\sqrt{10})K$ and $K = 0.4094$.

In each of the next two examples, the open-loop transfer function $KF(s)$ is unstable. In the first case there is a pole in the right half-plane, and in the second, a double pole at the origin. Such poles might be an unavoidable characteristic of one part of the system that cannot be changed. However, the other factors in $KF(s)$ allow the locus to move inside the left half-plane as K is increased.

► EXAMPLE 14.9

Show the root locus and find the values of K for which the overall system is stable when

$$KF(s) = \frac{K(s+2)}{s(s-1)}$$

Solution

The complete locus is shown in Figure 14.14. To find the point where the branches cross the imaginary axis, we can write $KF(j\omega) = -1$. Then $K(j\omega + 2) = -j\omega(j\omega - 1)$, so

$$2K = \omega^2 \quad (27a)$$

$$\omega K = \omega \quad (27b)$$

As expected, one solution is $\omega = 0$ and $K = 0$. For the other solution, $K = 1$ from (27b) and $\omega = \sqrt{2}$ from (27a). The system is stable for all $K > 1$.

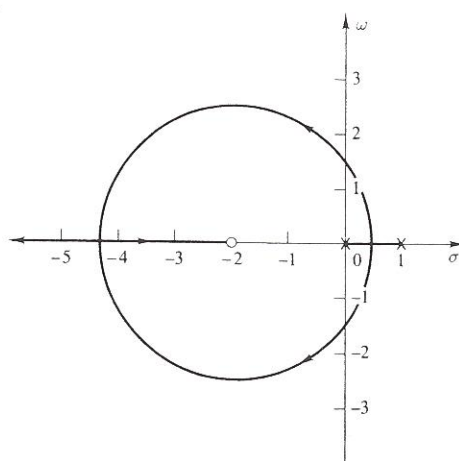


FIGURE 14.14 Root locus for Example 14.9.

► EXAMPLE 14.10

Find the root locus when

$$KF(s) = \frac{K(s+1)}{s^2(s+10)}$$

The double pole at the origin might come from an essential part of the open-loop system. The zero at $s = -1$ might have been added in order to move the locus to the left, but in practice the component that provided this zero might also have added an extra pole. In such a case, the pole can be placed far enough from the origin that it will not adversely affect the desired result.

Solution

The asymptotes corresponding to large values of K cross the axis at $\sigma_0 = (-10 + 1)/2 = -9/2$. The complete locus appears in Figure 14.15. It can be shown that two branches enter the real axis at $s = -5/2$ and that two branches leave the real axis at $s = -4$. If the pole of $KF(s)$ at $s = -10$ were moved considerably closer to the zero, then the branches leaving the double pole at the origin would not be drawn all the way to the real axis but would instead approach directly the asymptotes for large K .

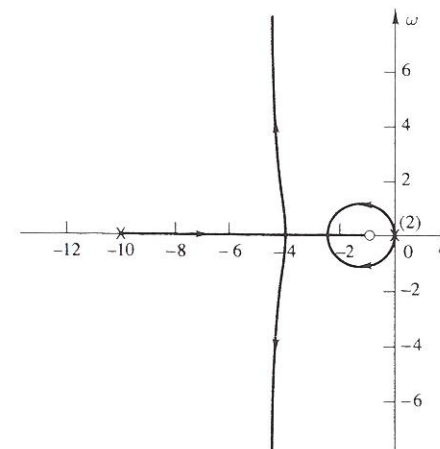


FIGURE 14.15 Root locus for Example 14.10.

The concepts that we have developed for the construction of a root locus can be extended to other situations. If the sign of the signal fed back to the summer in Figure 14.7 is changed from minus to plus, then the closed-loop transfer function is

$$T(s) = \frac{G(s)}{1 - G(s)H(s)}$$

By comparing this equation with (19) and (20), we see that the only change has been to replace K by $-K$. For this reason, we sometimes wish to

start with the pole-zero pattern of $KF(s)$ and then draw the root locus for negative values of K .

Root Locus For Negative Values of K

The locus is still symmetrical with respect to the real axis of the s -plane, and it still has one branch starting from each of the poles of $F(s)$. As the magnitude of K increases, the branches again either approach the finite-plane zeros of $F(s)$ or approach infinity. The asymptotes for those branches that approach infinity will still have equally spaced angles and will still meet at a point on the real axis given by (24). However, if there is an odd number of such asymptotes, one of them will be the positive (rather than the negative) real axis. A point on the real axis will belong to the locus if and only if the number of real poles and zeros to the right of that point is even (rather than odd).

Equation (21) is valid for both positive and negative values of K . Sometimes, however, people prefer to rewrite it specifically for negative values of K as

$$|K|F(s) = 1 \quad (28)$$

Equations (22) and (23) were written only for the case where K is restricted to positive values. The corresponding equations for negative values of K are

$$\arg F(s) = \pm n\pi \quad \text{for } n = 0, 2, 4, \dots$$

$$K = -\frac{1}{|F(s)|}$$

The applications for negative values of K are illustrated by a single example.

► EXAMPLE 14.11

Repeat Examples 14.3 and 14.4 for negative values of K . Recall that the open-loop transfer function is

$$KF(s) = \frac{K}{s^3 + 7s^2 + 14s + 8} = \frac{K}{(s+1)(s+2)(s+4)}$$

Solution

The parts of the real axis that belong to the locus are indicated by heavy lines in Figure 14.16. All three branches of the locus eventually go to infinity. The asymptotes still meet at $\sigma_0 = (-1 - 2 - 4)/3 = -7/3$, but one of them is now the positive real axis. The arrows on the locus indicate increasing magnitudes for the negative constant K .

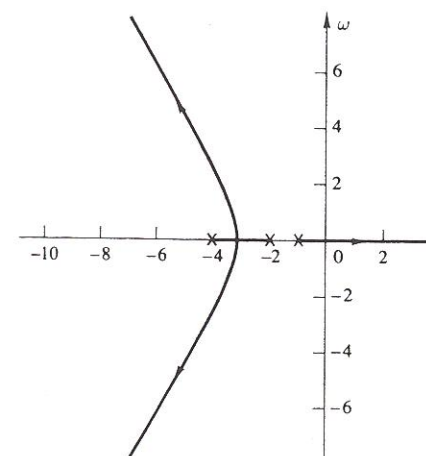


FIGURE 14.16 Root locus for Example 14.11.

In Example 14.4 we used (21) to write $KF(j\omega) = -1$, from which we obtained

$$\begin{aligned} K &= 7\omega^2 - 8 \\ 0 &= \omega(\omega^2 - 14) \end{aligned}$$

which are valid for both positive and negative values of K . The only solution for negative K is $\omega = 0$ and $K = -8$, which describes the point at which the right branch passes into the right half-plane. Thus the system is stable for $|K| < 8$. If we were to use (28) with s replaced by $j\omega$, we would get

$$\begin{aligned} |K| &= -7\omega^2 + 8 \\ 0 &= \omega(\omega^2 - 14) \end{aligned}$$

which yield the same result. Combining this solution with that for Example 14.4, we see that if K is allowed to have both positive and negative values, the condition for stability is $-8 < K < 90$.

Root Locus for Systems not in Standard Feedback Form

Our root-locus rules may be useful even when the system is not presented in the standard feedback configuration shown in Figure 14.7. We require only that the denominator of the overall transfer function be written in the form $1 + KF(s)$. Recall the mechanical system that is shown in Figure 14.6(a)

and considered in Example 14.2 and that has the transfer function

$$T(s) = \frac{1}{\frac{B}{M}s + \frac{K}{M} + s^2}$$

We want the locus of the poles of $T(s)$ when first K/M and then B/M are varied. To put the expression into a suitable form, we divide both halves of the fraction by those denominator terms that do not contain the parameter to be varied. Thus we write

$$T(s) = \frac{\frac{1/M}{s(s+B/M)}}{1 + \frac{K/M}{s(s+B/M)}} \quad (29a)$$

$$T(s) = \frac{\frac{1/M}{s^2 + K/M}}{1 + \frac{(B/M)s}{s^2 + K/M}} \quad (29b)$$

In each case, the denominator is in the right form. In (29a), we regard the open-loop transfer function as having poles at $s = 0$ and at $s = -B/M$, and we then draw the root locus as K/M is increased from zero to infinity. This gives the diagram that was shown in Figure 14.6(b).

Using (29b), we can define an open-loop transfer function that has poles at $s = \pm j\sqrt{K/M}$ and a zero at the origin. Drawing the locus as B/M increases from zero to infinity gives Figure 14.6(c).

■ 14.3 BODE DIAGRAMS

A designer often characterizes parts of a feedback control system by their sinusoidal-steady-state responses. The basic ideas were presented in Section 8.5 and can be summarized by (8.44), (8.49), and (8.51). We shall start this section with these same equations. However, we shall use $T(s)$ rather than $H(s)$ for a general transfer function in order to avoid confusion with the use of $H(s)$ for the feedback transfer function in feedback systems. To obtain an expression for the frequency-response function $T(j\omega)$, we replace s by $j\omega$ in $T(s)$ and then write the resulting complex quantity in polar form as

$$T(j\omega) = M(\omega)e^{j\theta(\omega)} \quad (30)$$

where $M(\omega)$ is the magnitude of $T(j\omega)$ and $\theta(\omega)$ is its angle. If the input of a stable system is the sinusoidal function

$$u(t) = \sin \omega t \quad (31)$$

then the steady-state response is

$$y_{ss}(t) = M \sin(\omega t + \theta) \quad (32)$$

More generally, the steady-state response to the sinusoidal input $u(t) = B \sin(\omega t + \phi_1)$ is

$$y_{ss}(t) = BM \sin(\omega t + \phi_1 + \theta)$$

If we draw curves of $M(\omega)$ and $\theta(\omega)$ versus ω , we can see how the magnitude and angle of the steady-state response change as the frequency of the input is changed, as was illustrated in Section 8.5. However, it is often more useful to express the magnitude of $T(j\omega)$ in decibels, to use semilog paper, and to present the two curves in the form of a Bode diagram.

Bode diagrams have several advantages. A wide range of values of $M(\omega)$ and of ω can be included (although the point corresponding to $\omega = 0$ can never be shown because of the logarithmic frequency scale). A number of rules can be developed to enable a designer quickly to sketch reasonable approximations to the Bode diagrams, although we shall emphasize computer-generated plots. Conversely, the transfer function $T(s)$ can be approximated from Bode diagrams that have been constructed from experimental measurements. For subsystems in series, the corresponding Bode diagrams can be added to obtain the diagram for the combination. For feedback systems, the diagrams for the open-loop transfer function provide important information about the stability of the overall systems.

To express a real, positive, dimensionless quantity in decibels (usually abbreviated dB), we take its logarithm (to the base 10) and then multiply by 20. Thus

$$M(\omega)|_{dB} = 20 \log_{10} M(\omega) \quad (33)$$

Note that the decibel gain $M(\omega)|_{dB}$ is positive when $M(\omega) > 1$ and negative when $M(\omega) < 1$. When the magnitude of the transfer function is 1, 10, 100, and 1000, respectively, the corresponding decibel gain is 0, 20, 40, and 60.

Construction of Bode Diagrams

We begin the discussion by presenting several simple cases. The diagrams can easily be drawn by hand and turn out to be important to understanding the asymptotic behavior in more complicated cases. Keep in mind that the ω scale is logarithmic and that the curves are drawn on semilog paper. Unless otherwise stated, any gain constant K is assumed to be a positive number.

► EXAMPLE 14.12

Construct the magnitude curve for each of the following frequency-response functions: $T_1(j\omega) = K$, $T_2(j\omega) = j\omega K$, $T_3(j\omega) = K/j\omega$, and $T_4(j\omega) = K/(j\omega)^2$. Because all of the angle functions turn out to be constants in this example, we shall not plot the angle curves.

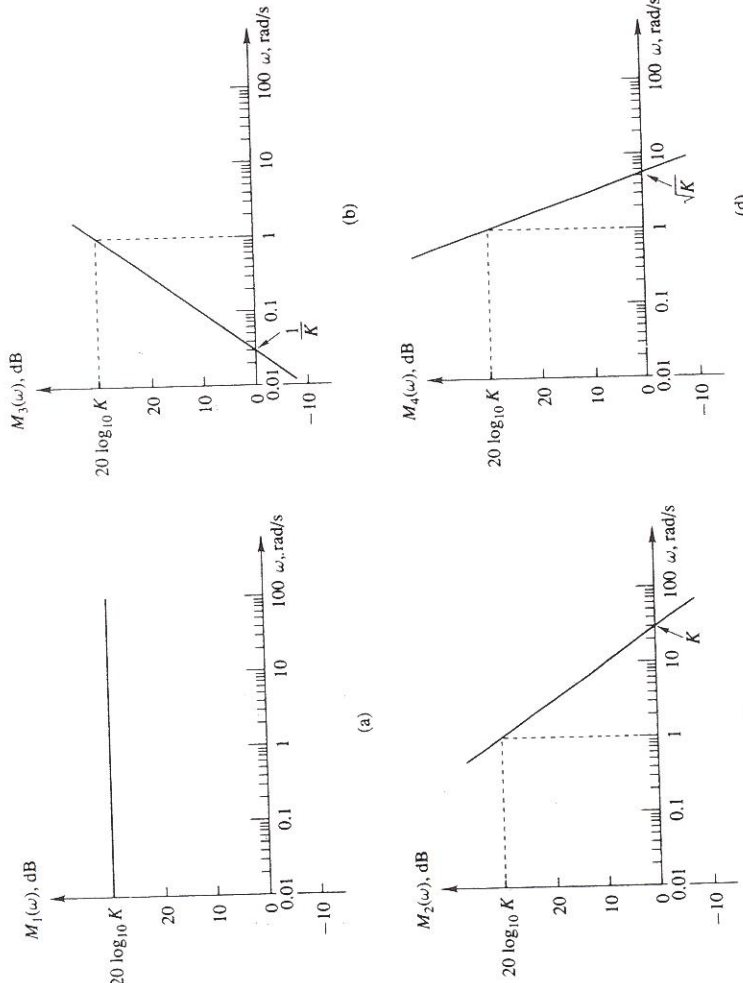


FIGURE 14.17 Magnitude curves for Example 14.12. (a) $T_1(j\omega) = K$. (b) $T_2(j\omega) = j\omega K$. (c) $T_3(j\omega) = K/(j\omega)$. (d) $T_4(j\omega) = K/(j\omega)^2$.

Solution

For $T_1(j\omega) = K$, $M_1(\omega)|_{dB} = 20 \log_{10} K$, which gives the horizontal line shown in Figure 14.17(a). The angle $\theta_1(\omega)$ is zero for all values of ω .

For $T_2(j\omega) = j\omega K$, we can write $M_2(\omega)|_{dB} = 20 \log_{10} \omega K = 20 \log_{10} K + 20 \log_{10} \omega$, which describes the straight line shown in Fig. 14.17(b). The slope of the line is usually expressed in units of decibels per decade or decibels per octave. A decade corresponds to increasing the frequency by a multiplying factor of 10, an octave to doubling the frequency. For this part of the example, when the frequency is increased from ω_a to $10\omega_a$ the resulting magnitude change is

$$20 \log_{10}(10\omega_a K) - 20 \log_{10}(\omega_a K) = 20 \log_{10} 10 = 20 \text{ dB}$$

If we double the frequency, the magnitude change is

$$20 \log_{10}(2\omega_a K) - 20 \log_{10}(\omega_a K) = 20 \log_{10} 2 \simeq 6 \text{ dB}$$

Thus the slope of the line in Figure 14.17(b) is 20 dB per decade and 6 dB per octave. The angle $\theta_2(\omega)$ is 90° for all values of ω .

For $T_3(j\omega) = K/(j\omega)$, we have $M_3(\omega)|_{dB} = 20 \log_{10}(K/\omega) = 20 \log_{10} K - 20 \log_{10} \omega$, which describes a straight line with a slope of -20 dB per decade, as shown in part (c) of the figure. The angle $\theta_3(\omega)$ is -90° for all values of ω .

For the general case where $T(j\omega) = K/(j\omega)^n$, we see that

$$M(\omega)|_{dB} = 20 \log_{10}(K/\omega^n) = 20 \log_{10} K - 20n \log_{10} \omega$$

Then the magnitude curve is a straight line with a slope of $-20n$ dB per decade, and the angle is a constant $-90n^\circ$. Similarly, if $T(j\omega) = K(j\omega)^n$, the magnitude curve has a slope of $+20n$ dB per decade, and the angle curve is $+90n^\circ$.

The results of the last example will be important when we draw the low- and high-frequency asymptotes for more complicated functions. For very small or very large values of ω , frequency-response functions usually reduce to the cases examined in Example 14.12. Remember that the slope of the magnitude curve is $-20n$ dB per decade for $T(j\omega) = K/(j\omega)^n$ and is $+20n$ dB per decade for $T(j\omega) = (j\omega)^n K$. In addition to the slope, we shall need to locate one point on these magnitude curves. One way to do so (illustrated in Figure 14.17) is to note that when $\omega = 1$, $M(\omega)|_{dB} = 20 \log_{10} K$. Another easy way is to note that the line (extended if necessary) crosses the zero-dB axis when $|T(j\omega)| = 1$. For $T(j\omega) = K/(j\omega)^n$, this occurs when $\omega = \sqrt[n]{K}$; for $T(j\omega) = (j\omega)^n K$, it occurs when $\omega = \sqrt[n]{1/K}$.

The next three examples provide additional background for understanding the construction of Bode diagrams for cases of arbitrary complexity. Following these examples, we shall discuss briefly a general method for drawing approximate curves for any transfer function, even though our emphasis will be on the use of computer-generated plots.

► **EXAMPLE 14.13**

Construct the Bode diagram for $T(s) = 1/(1 + \tau s)$ by examining the frequency-response function

$$T(j\omega) = \frac{1}{1 + j\omega\tau} \quad (34)$$

Solution

The computer-generated curves are shown in Figure 14.18. For very small values of ω , $T(j\omega)$ approaches 1, so the magnitude curve approaches a constant value of 0 dB, and the angle curve approaches 0°. At very high frequencies, where $\omega\tau \gg 1$, $T(j\omega)$ approaches $1/(j\omega\tau)$. From the previous example, the high-frequency asymptote for the magnitude curve has a slope of -20 dB per decade and crosses the zero-dB axis at $\omega = 1/\tau$. The curve of $\theta(\omega)$ must approach -90° for large values of ω .

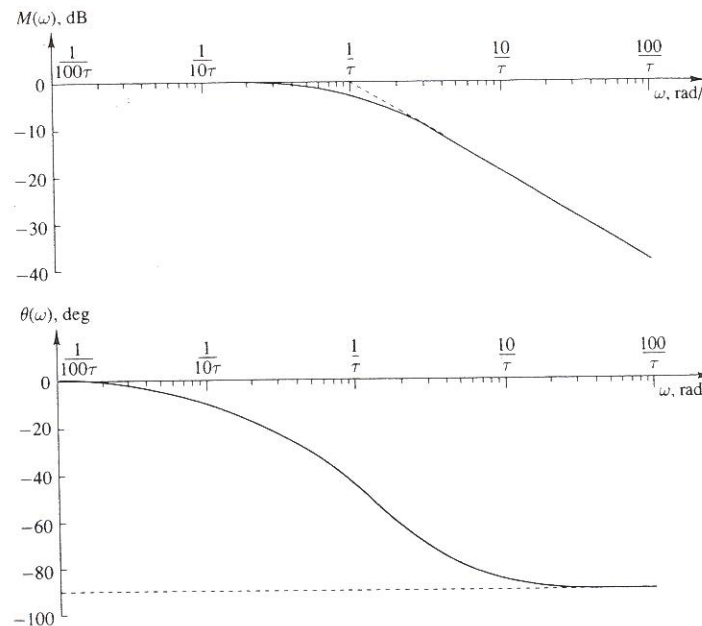


FIGURE 14.18 Bode diagram for $T(s) = 1/(1 + \tau s)$.

In part (a) of the figure, note that the low- and high-frequency asymptotes meet at $\omega = 1/\tau$, which is sometimes called the **corner frequency** or **break frequency**. Together, these asymptotes could serve as a rough approximation to the exact curve, especially if correction factors were used

near the break frequency. Although we shall rely on computer-generated plots, the references in Appendix D contain further guidelines that enable a designer to draw approximate curves quickly.

► **EXAMPLE 14.14**

Suppose that two frequency-response functions are related by the equation

$$T_2(j\omega) = \frac{1}{T_1(j\omega)}$$

and that the Bode diagram for $T_1(j\omega)$ is available. Develop a procedure for constructing the diagram for $T_2(j\omega)$.

Solution

If $T_1(j\omega) = M_1(\omega)e^{j\theta_1(\omega)}$, then

$$T_2(j\omega) = \frac{1}{M_1(\omega)}e^{-j\theta_1(\omega)}$$

and we see that $M_2(\omega) = 1/M_1(\omega)$ and $\theta_2(\omega) = -\theta_1(\omega)$. Thus the new angle curve is just the negative of the original one. Furthermore,

$$\begin{aligned} M_2(\omega)|_{\text{dB}} &= 20 \log_{10}[1/M_1(\omega)] \\ &= -20 \log_{10}M_1(\omega) = -M_1(\omega)|_{\text{dB}} \end{aligned}$$

so the new magnitude curve is also the negative of the original one. As a specific example, we can use the results of Example 14.13 to draw immediately the curves shown in Figure 14.19 for $T(j\omega) = 1 + j\omega\tau$.

► **EXAMPLE 14.15**

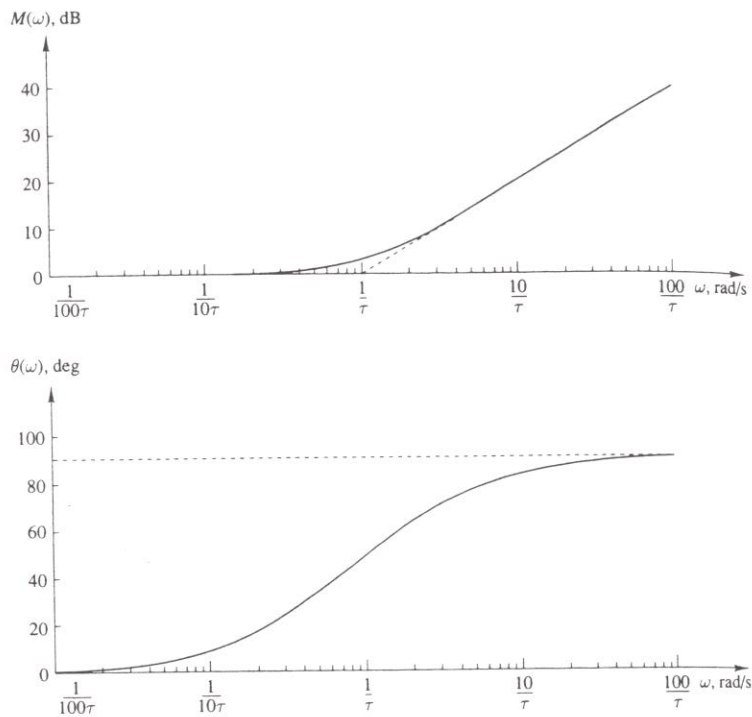
Construct the Bode diagram for $T(s) = \omega_n^2/(s^2 + 2\xi\omega_n s + \omega_n^2)$, for which

$$T(j\omega) = \frac{\omega_n^2}{-\omega^2 + j(2\xi\omega_n)\omega + \omega_n^2} = \frac{1}{1 + j2\xi(\omega/\omega_n) - (\omega/\omega_n)^2} \quad (35)$$

Solution

The complete magnitude and angle curves when the damping ratio $\xi = 1$, 0.5, and 0.1 are shown in Figure 14.20. Note that in order to make the curves more generally applicable, we have made the abscissa the normalized frequency ω/ω_n .

From (35), we see that for very small values of ω , $T(j\omega)$ approaches 1. Thus the low-frequency asymptotes are 0 dB and 0°. For large values of ω , $T(j\omega)$ approaches $1/(j\omega/\omega_n)^2$. Then the high-frequency magnitude asymptote must have a slope of -40 dB per decade and must cross the

FIGURE 14.19 Bode diagram for $T(s) = 1 + \tau s$.

zero-dB axis at $\omega = \omega_n$. The high-frequency asymptote for the angle is -180° .

We could try to approximate the magnitude curve in part (a) of the figure by using only the low- and high-frequency asymptotes. If we do this, however, very large errors could occur near the break frequency, especially if ζ is very small. Special correction curves would usually be required.

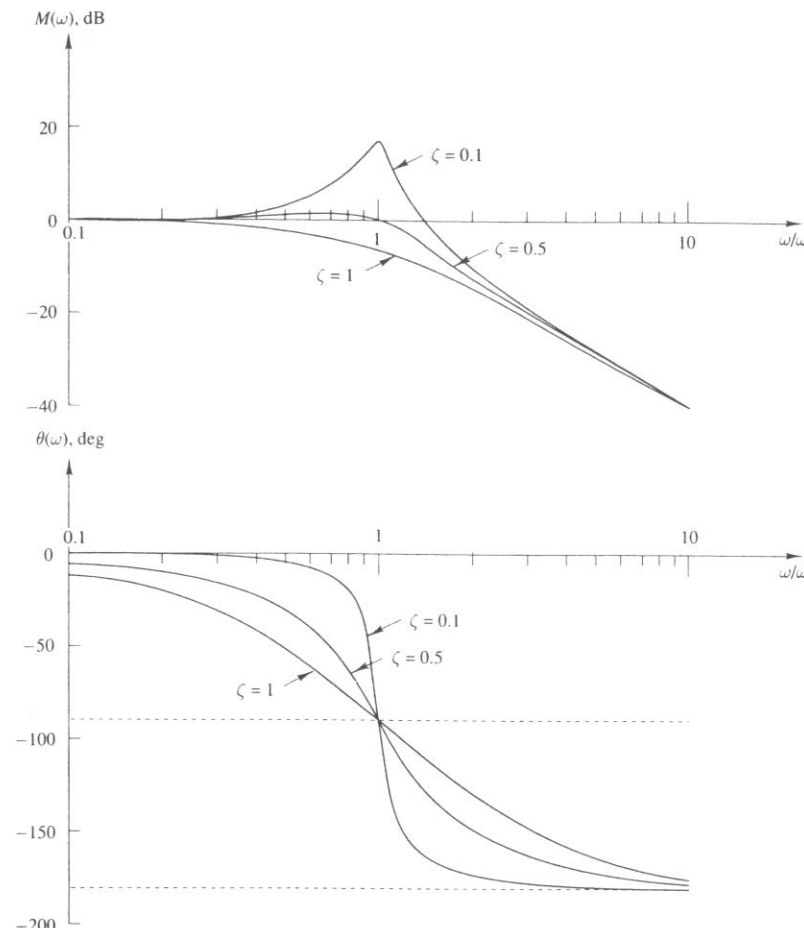
Frequently it is desirable to express a transfer function as the product of several factors. For example, let

$$T(s) = T_1(s)T_2(s)T_3(s) \quad (36)$$

in which case

$$T(j\omega) = T_1(j\omega)T_2(j\omega)T_3(j\omega) \quad (37)$$

Using the appropriate subscripts, we let $M(\omega)$ and $\theta(\omega)$ denote the magnitude and angle of the individual frequency-response functions in the

FIGURE 14.20 Bode diagram for $T(s) = \omega_n^2/(s^2 + 2\zeta\omega_n s + \omega_n^2)$.

usual way. By the rules for complex numbers, we can write, for the overall function $T(j\omega)$,

$$M(\omega) = M_1(\omega)M_2(\omega)M_3(\omega) \quad (38a)$$

$$\theta(\omega) = \theta_1(\omega) + \theta_2(\omega) + \theta_3(\omega) \quad (38b)$$

Furthermore, $M(\omega)|_{dB} = 20 \log_{10}[M_1(\omega)M_2(\omega)M_3(\omega)]$, so

$$M(\omega)|_{dB} = M_1(\omega)|_{dB} + M_2(\omega)|_{dB} + M_3(\omega)|_{dB} \quad (39)$$

Thus the individual magnitude curves can be added, as can the individual angle curves.

One application of (38b) and (39) occurs when a block diagram contains several blocks in series. The overall transfer function for the partial diagram in Figure 14.21 is given by (36). To construct the Bode diagram for the overall frequency-response function, we merely add the magnitude and angle curves for the individual blocks.

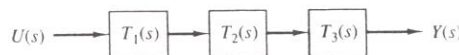


FIGURE 14.21 Blocks in series corresponding to (36).

As will be discussed in Section 14.4, it is sometimes necessary to insert additional components in series with the original open-loop system in order to meet the design specifications. Using (38b) and (39) enables us to determine, for these additional components, the magnitude and angle characteristics needed in order to allow the complete Bode diagram to be appropriately modified.

Suppose that we have a transfer function in factored form. For any real poles or zeros, we would have factors of the form $s + \alpha$ in the denominator or numerator. A quadratic factor corresponding to a pair of complex poles or zeros inside the left half-plane would have the form $s^2 + 2\xi\omega_n s + \omega_n^2$, where $0 < \xi < 1$. Thus a typical transfer function might be

$$T(s) = \frac{K(s + \alpha)}{s(s + \beta)(s^2 + 2\xi\omega_n s + \omega_n^2)}$$

which we can rewrite as

$$T(s) = \left(\frac{\alpha K}{\beta\omega_n^2}\right) \left(\frac{1}{s}\right) \left(1 + \frac{s}{\alpha}\right) \left(\frac{1}{1 + s/\beta}\right) \left(\frac{\omega_n^2}{s^2 + 2\xi\omega_n s + \omega_n^2}\right)$$

When s is replaced by $j\omega$ to give the frequency-response function $T(j\omega)$, we can see that each of the factors was among those treated in the previous examples. The magnitude curve for the constant $\alpha K / \beta\omega_n^2$ is a horizontal line, and the angle is zero. Corresponding to the factor $1/s$, we have a magnitude curve with a slope of -20 dB per decade and an angle of -90° . The curves for the final three factors are similar to those in Figures 14.19, 14.18, and 14.20, respectively. The magnitude and angle curves for $T(j\omega)$ can be found by adding the individual curves.

This approach is especially useful when we draw approximate curves by hand. However, we shall generally use computer-generated curves, in which case there is no need to break the transfer function up into individual factors.

Stability Criteria

Consider again the standard feedback configuration that is shown in Figures 13.22(a) and 14.7 and is repeated in Figure 14.22. We discussed in Section 14.2 the importance of being able to predict the nature of the free response of the overall system from a knowledge of the open-loop transfer function $G(s)H(s)$. If the behavior of the overall system needs to be modified, we can consider changing the gain constant associated with $G(s)H(s)$ or can even arrange to give it additional poles and zeros.

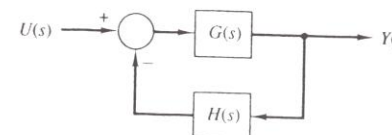


FIGURE 14.22 Block diagram of a feedback system.

The most fundamental way of relating the frequency-response function $G(j\omega)H(j\omega)$ to the stability of the overall system is to construct a polar plot. We would regard $G(j\omega)H(j\omega)$ as a vector drawn from the origin of a new complex plane (different from the s -plane) and would look at the path traced out by the tip of that vector as ω increases. A test known as the **Nyquist stability criterion** can be applied to determine whether the system is stable. Furthermore, that test can give considerable insight into whether the system will remain stable even if some of the characteristics of the open-loop transfer function undergo moderate changes.

Knowledge of the Nyquist criterion is necessary for a complete understanding of how the Bode diagram for $G(s)H(s)$ can be related to the stability of the overall system. Unfortunately, developing the Nyquist criterion is fairly involved, so we must refer those interested in it to the references in Appendix D. In the following discussion, we shall assume that all the poles of the open-loop transfer function are inside the left half-plane, except for a possible first-order pole at the origin. Then we can state, without proof, the following definitions and properties.

The Bode diagram in Figure 14.23 represents the open-loop transfer function $G(s)H(s)$. The frequency at which the magnitude curve crosses the zero-dB line is denoted by ω_{pm} and is sometimes called the **magnitude crossover frequency**. The **phase margin** ϕ_m is the amount by which the angle curve would have to be moved down in order to make the angle $\theta(\omega_{pm})$ be -180° .

The frequency at which the angle curve crosses -180° , sometimes called the **phase crossover frequency**, is denoted by ω_{gm} . The **gain margin** k_m is the number of decibels by which the magnitude curve would have to be moved up in order to make $M(\omega_{gm})|_{dB} = 0$. The gain and phase margins are

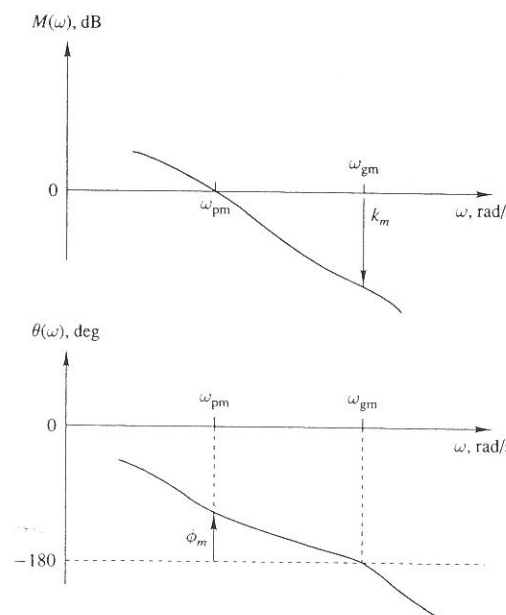


FIGURE 14.23 Bode diagram showing the phase margin ϕ_m and the gain margin k_m .

labeled in Figure 14.23. For the overall system to be stable, both the gain margin and the phase margin must be positive, as is assumed in the figure.

There are no standard symbols for the gain and phase margins or for the frequencies at which these quantities are measured. The subscripts we have used in the symbols ω_{pm} and ω_{gm} indicate the frequencies at which the phase margin and gain margin, respectively, are measured. Although the nature of the plots in Figure 14.23 is fairly typical, cases exist for which our definitions of k_m and ϕ_m do not apply. For example, it is possible for the curve of $\theta(\omega)$ never to cross the -180° axis or to cross it more than once. Similarly, the curve of $M(\omega)|_{\text{dB}}$ could cross the zero-dB axis more than once.

In order for the closed-loop system not to be too lightly damped and in order to be sure that it will remain stable even if there are some variations in the parameters, a designer would insist on certain minimum values for the gain and phase margins. The ranges of desired gain and phase margins depend on the particular system being considered and on the intended applications. However, a gain margin of about 10 dB and a phase margin of 45° are typical for many systems.

Increasing the phase margin generally increases the damping ratio ξ associated with a pair of complex poles. For specific second-order systems,

explicit relationships between ϕ_m and ξ can be derived. Some of the references in Appendix D contain curves of ξ versus ϕ_m , but it is important to note the specific open-loop transfer function for which they apply.

In order to give some plausibility to the foregoing statements about the gain and phase margin, let us look at the steady-state behavior of the feedback system in Figure 14.22 when the input is sinusoidal. At the frequency ω_{gm} , the angle of the open-loop transfer function is -180° . Because of the signs shown on the summer, the signal fed back from the $G(s)H(s)$ path is then in phase with the input and adds directly to it.

Suppose the input is now removed. If the magnitude of the open-loop gain is less than unity at the frequency ω_{gm} , then the signal fed back to the summer continually diminishes, and the output goes to zero. If $|M(\omega_{gm})| = 1$, corresponding to 0 dB, the signal fed back to the summer is just large enough to sustain the sinusoidal oscillations at a constant amplitude. Such a condition describes a marginally stable system. If $|M(\omega_{gm})| > 1$, then the oscillations continually grow in magnitude, and the system is unstable.

A positive gain margin means that $M(\omega_{gm})|_{\text{dB}} < 0$, corresponding to a stable system. A gain margin of zero occurs when $M(\omega_{gm})|_{\text{dB}} = 0$. A negative gain margin means that $M(\omega_{gm})|_{\text{dB}} > 0$, corresponding to an unstable system.

The MATLAB computer program can not only yield the Bode diagram for a given open-loop transfer function but can also list the gain and phase margins and the frequencies at which they are measured. The gain margin can be expressed both in decibels and as the additional multiplying factor needed to make $M(\omega_{gm}) = 1$. As in any computer program that produces a smooth curve from discrete numerical calculations, values corresponding to special points on the curve are only approximations to the exact numbers. Although a designer would require only reasonably close answers, more accurate values can always be achieved by increasing the number of points at which calculations are made. We now make use of MATLAB to draw and interpret the Bode diagram for the system that was considered in Examples 14.3 and 14.4.

► EXAMPLE 14.16

Draw the Bode diagram for the open-loop transfer function

$$G(s)H(s) = \frac{K}{(s+1)(s+2)(s+4)} = \frac{K/8}{(1+s)(1+s/2)(1+s/4)}$$

when $K = 20$. Find the gain and phase margins. Determine the values of the positive constant K for which the closed-loop transfer function is stable.

Solution

Although we could add the magnitude and angle curves for $K/8$, $1/(1+j\omega/2)$, $1/(1+j\omega/4)$, and $1/(1+j\omega/8)$ in order to construct the diagram for

$G(j\omega)H(j\omega)$, we use MATLAB to obtain the plots shown in Figure 14.24. The gain and phase margins are shown in the figure. Their numerical values are $k_m = 13.13$ dB (corresponding to a multiplying factor of 4.535, where $13.13 = 20 \log_{10} 4.535$) and $\phi_m = 64.1^\circ$. Other values of interest are $\omega_{gm} = 3.75$ rad/s and $\omega_{pm} = 1.54$ rad/s.

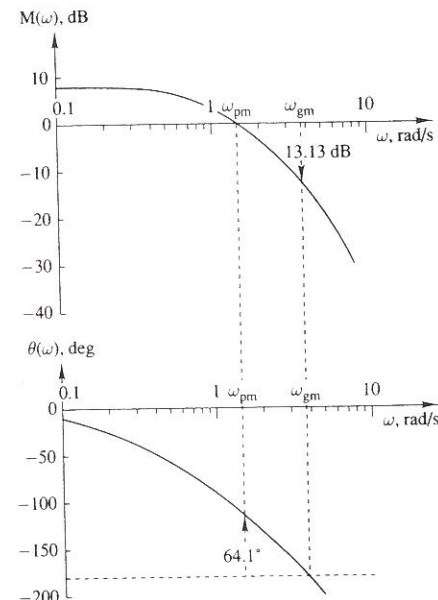


FIGURE 14.24 Bode diagram for Example 14.16.

Multiplying the transfer function by a positive constant A raises the magnitude curve by the constant $20\log_{10}A$ without changing the angle curve. For a marginally stable system, $k_m = 0$ dB. In our case this would correspond to $A = 4.535$ and to a value of $K = 4.535 \times 20 = 90.70$. This is in reasonable agreement with the result of Example 14.4, where we found from the root-locus magnitude criterion that the overall system is stable for gains in the interval $0 < K < 90$.

■ 14.4 DESIGN GUIDELINES

The block diagram for a basic feedback configuration is shown in Figure 14.25(a). Particular systems may have more complicated diagrams with a number of additional feedback and feedforward paths. However, many

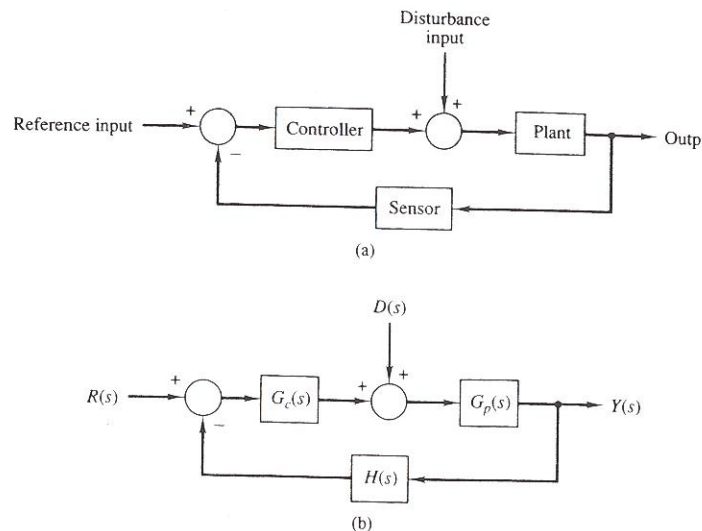


FIGURE 14.25 Block diagrams for a basic feedback system.

diagrams can be reduced to the one in the figure, and analyzing it will provide an introduction to some of the design techniques most often used.

The **plant** is the system to be controlled. It may contain almost any collection of linearized components or processes, and its parameters are generally already fixed and beyond the designer's control. The purpose of the **sensor** is to measure the output and feed a signal back to the input summing device. The engineer may also choose to add other components within the sensor block to improve the system performance. The **controller** not only provides the excitation for the plant but also can be designed to meet the specifications for the overall system behavior. Its characteristics and implementation are chosen by the engineer.

The notation that we shall use is shown in Figure 14.25(b). The transfer functions for the controller, plant, and sensor are denoted by $G_c(s)$, $G_p(s)$, and $H(s)$, respectively. Because the diagram has two inputs, we distinguish their Laplace transforms by using $R(s)$ for the reference input and $D(s)$ for the disturbance input. We assume that we want the output $y(t)$ to follow closely any changes in the reference input $r(t)$. For the system examined in Section 14.1, the input and output variables were the angular displacements of mechanical components. However, they might equally well be any other type of variable.

A system may be subjected to unpredictable disturbances that tend to affect the output adversely. Examples include wind gusts on a moving vehicle and a load torque exerted on a rotating shaft to which a cutting tool

is attached. Such unwanted inputs are usually exerted directly on the plant and are represented in the figure by the transformed variable $D(s)$. We want the output to be relatively insensitive to a disturbance input. An additional concern, which we shall discuss only in a qualitative way, is the need for the system's behavior to remain acceptable even if some of its parameters undergo moderate changes or if random noise signals arise within the system.

We define the following two transfer functions for the system shown in Figure 14.25(b): $T_R(s) = Y(s)/R(s)$ when the disturbance input $D(s)$ is zero, and $T_D(s) = Y(s)/D(s)$ when the reference input $R(s)$ is zero. By (13.46),

$$T_R(s) = \frac{Y(s)}{R(s)} = \frac{G_c(s)G_p(s)}{1 + G_c(s)G_p(s)H(s)} \quad (40a)$$

$$T_D(s) = \frac{Y(s)}{D(s)} = \frac{G_p(s)}{1 + G_c(s)G_p(s)H(s)} \quad (40b)$$

We would of course like $T_R(s)$ to approach unity and $T_D(s)$ to approach zero. Because both transfer functions have the same denominator, they will have the same poles. Thus consideration of stability and consideration of the form of the transient response will yield the same results, no matter which of the two functions is used. Information about these items can be obtained from root-locus or Bode plots corresponding to the open-loop transfer function $G_c(s)G_p(s)H(s)$.

One design criterion is the steady-state response to common reference inputs, such as the unit step function. Because we want the output to follow the reference input, we define the error function

$$e(t) = r(t) - y(t) \quad (41)$$

which, when transformed, gives

$$E(s) = R(s) - Y(s)$$

For the special case where $H(s) = 1$, $E(s)$ is the transformed output of the first summer and the input to the controller. For the general case, however, $E(s)$ does not appear in the block diagram.

When examining steady-state responses, we can apply the final-value theorem, which was presented in (7.83) and is repeated here:

$$f(\infty) = \lim_{s \rightarrow 0} sF(s) \quad (42)$$

provided that $sF(s)$ has no poles on the imaginary axis or in the right half of the complex plane. We can also write a partial-fraction expansion, omitting those terms that do not contribute to the steady-state response.

In order to investigate the effects of different types of controllers, we shall use for purposes of illustration the following second-order transfer function for the plant:

$$G_p(s) = \frac{K_p}{(s+a)(s+b)} \quad (43)$$

where a and b are nonnegative real constants. For the servomechanism treated in Section 14.1, the transfer function of the motor had this form with $a = 0$, $b = 1/\tau_m$, and $K_p = K_m$. If we include an input for the hydraulic system shown in Figure 12.13, it will have a transfer function similar to (43) with real positive values for a and b .

In the ensuing discussion, we shall also let $H(s) = 1$. Then the system diagram in Figure 14.25(b) reduces to the one in Figure 14.26, for which

$$T_R(s) = \frac{G_c(s) \frac{K_p}{(s+a)(s+b)}}{1 + G_c(s) \frac{K_p}{(s+a)(s+b)}} \quad (44a)$$

$$T_D(s) = \frac{\frac{K_p}{(s+a)(s+b)}}{1 + G_c(s) \frac{K_p}{(s+a)(s+b)}} \quad (44b)$$

where the open-loop transfer function is

$$\frac{K_p G_c(s)}{(s+a)(s+b)}$$

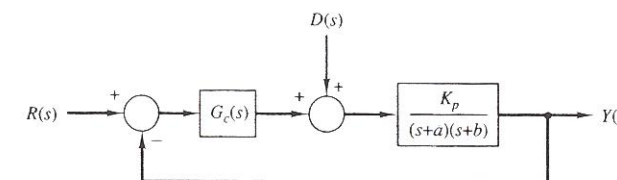


FIGURE 14.26 Block diagram for second-order plant and unity feedback.

Proportional Control

We first let $G_c(s)$ be the positive constant K_c . Then (44) reduces to

$$T_R(s) = \frac{\frac{K_c K_p}{(s+a)(s+b)}}{1 + \frac{K_c K_p}{(s+a)(s+b)}} = \frac{K_c K_p}{s^2 + (a+b)s + (ab + K_c K_p)} \quad (45a)$$

$$T_D(s) = \frac{\frac{K_p}{(s+a)(s+b)}}{1 + \frac{K_c K_p}{(s+a)(s+b)}} = \frac{K_p}{s^2 + (a+b)s + (ab + K_c K_p)} \quad (45b)$$

When the disturbance input is zero and the reference input is the unit step function, $R(s) = 1/s$ and

$$Y(s) = \frac{K_c K_p}{s[s^2 + (a+b)s + (ab + K_c K_p)]}$$

By the final-value theorem, the steady-state response is

$$y_{ss} = \frac{K_c K_p}{ab + K_c K_p} \quad (46)$$

The steady-state error is

$$e_{ss} = 1 - \frac{K_c K_p}{ab + K_c K_p} = \frac{ab}{ab + K_c K_p} \quad (47)$$

Although this is not zero, it can be made small by choosing K_c such that $K_c K_p \gg ab$.

The step input $r(t)$ and a possible curve for the output $y(t)$ are shown in Figure 14.27(a). The nature of the transient response depends on the poles of the closed-loop transfer function $T_R(s)$, which for the plot shown have been assumed to be on the negative real axis.

We next let the reference input be the unit ramp function

$$r(t) = \begin{cases} 0 & \text{for } t \leq 0 \\ t & \text{for } t > 0 \end{cases} \quad (48)$$

If $r(t)$ and $y(t)$ are angular displacements of rotating mechanical components, then the input in (48) corresponds to a constant angular velocity of 1 for all $t > 0$. Then $R(s) = 1/s^2$ and

$$Y(s) = \frac{K_c K_p}{s^2[s^2 + (a+b)s + (ab + K_c K_p)]}$$

for which the beginning of the partial-fraction expansion is

$$Y(s) = \frac{K_c K_p/(ab + K_c K_p)}{s^2} + \dots$$

so that

$$y(t) = \frac{K_c K_p}{ab + K_c K_p} t + \dots \quad (49)$$

The dots represent terms that are either constant or decaying with time. Thus for large values of time, $y(t)$ approaches a straight line with a slope of $K_c K_p/(ab + K_c K_p)$. For any finite value of $K_c K_p$, this slope will be less than 1, and the error will continually increase, as shown in Figure 14.27(b). For a rotating mechanical system, this means that the steady-state output angular velocity is less than that for the input, so the output angular displacement lags further and further behind the input. This lag can be reduced by making K_c very large.

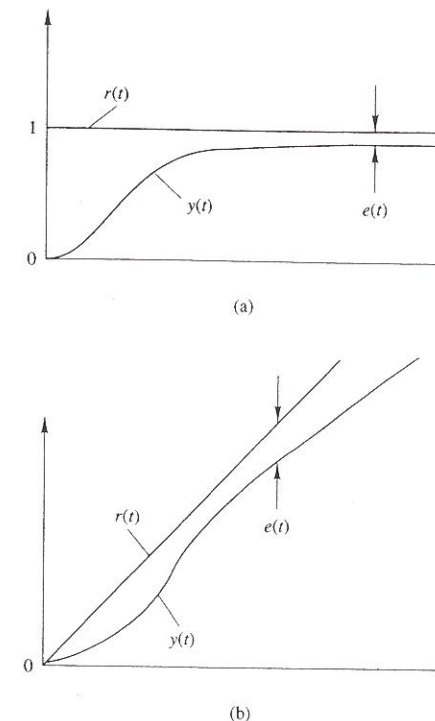


FIGURE 14.27 Response to the reference input when $G_c(s) = K_c$. (a) Unit step response. (b) Unit ramp response.

We consider next the response to an unwanted disturbance input. If $r(t) = 0$ and $d(t)$ is the unit step function, then $D(s) = 1/s$,

$$Y(s) = \frac{K_p}{s[s^2 + (a+b)s + (ab + K_c K_p)]}$$

and

$$y_{ss} = \frac{K_p}{ab + K_c K_p} \quad (50)$$

For the disturbance response to be small, we require $K_c \gg K_p$. Once again, we see that a large controller gain will improve the steady-state response. The reader may wish to show that if $d(t)$ is the unit ramp function, then

$$Y(s) = \frac{K_p}{s^2[s^2 + (a+b)s + (ab + K_c K_p)]}$$

and

$$y(t) = \frac{K_p}{ab + K_c K_p} t + \dots \quad (51)$$

which again indicates the need for a large value of K_c .

We now look at the nature of the transient response, which is governed by the poles of the closed-loop transfer function. These are points on the root locus that corresponds to the open-loop transfer function

$$\frac{K_c K_p}{(s+a)(s+b)}$$

and is shown in Figure 14.28. As long as a , b , and $K_c K_p$ are positive numbers, the system is always stable because the locus remains in the left half-plane. For large values of $K_c K_p$, however, the roots will be complex and far from the real axis, corresponding to a small damping ratio ζ . The transient response will then contain stronger oscillations than would normally be desired.

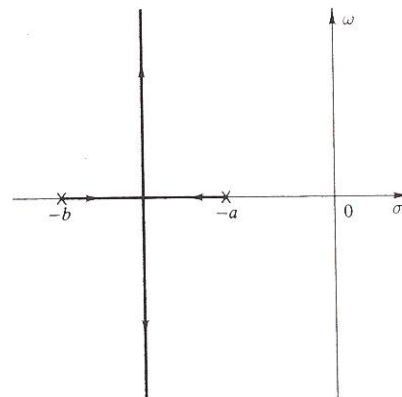


FIGURE 14.28 Root locus when $G_c(s) = K_c$.

Note that there are conflicting priorities concerning the choice of the controller gain K_c . For the best steady-state behavior, the gain should be very large. However, this can result in an undesirable transient response.

A typical Bode diagram is sketched in Figure 14.29. The magnitude curve has an initial slope of zero and a final slope of -40 dB per decade. As expected, the phase margin ϕ_m is always positive. Increasing $K_c K_p$ raises the magnitude curve without affecting the phase angle. This improves the steady-state behavior of the system but decreases ϕ_m . The gain margin k_m is not defined, because the angle curve never crosses -180° .

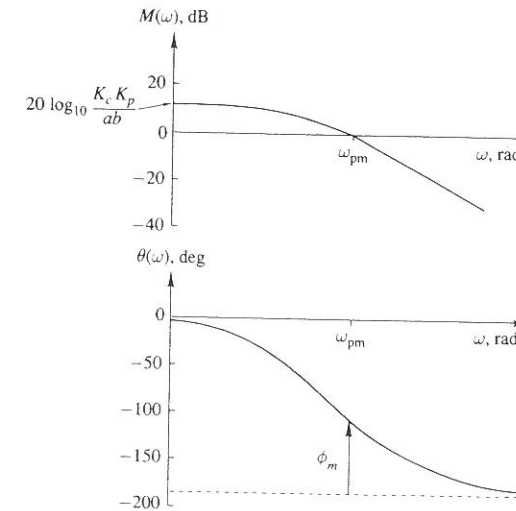


FIGURE 14.29 Bode diagram when $G_c(s) = K_c$.

Proportional-Plus-Derivative Control

We now take the controller's transfer function to be

$$G_c(s) = K_c(1 + K_D s) \quad (52)$$

Because the transfer function for a component described by $y(t) = K_D \dot{x}$ is $K_D s$, the controller includes both proportional and derivative action. Equations (44) become

$$\begin{aligned} T_R(s) &= \frac{\frac{K_c K_p (1 + K_D s)}{(s+a)(s+b)}}{1 + \frac{K_c K_p (1 + K_D s)}{(s+a)(s+b)}} \\ &= \frac{K_c K_p (1 + K_D s)}{s^2 + (a+b + K_c K_p K_D)s + (ab + K_c K_p)} \end{aligned} \quad (53)$$

and

$$\begin{aligned} T_D(s) &= \frac{\frac{K_p}{(s+a)(s+b)}}{1 + \frac{K_c K_p (1 + K_D s)}{(s+a)(s+b)}} \\ &= \frac{K_p}{s^2 + (a+b + K_c K_p K_D)s + (ab + K_c K_p)} \end{aligned} \quad (54)$$

We can examine the steady-state responses to the reference and disturbance inputs by the procedure used for the proportional controller. Because K_D does not affect the limit of $T_R(s)$ or $T_D(s)$ as $s \rightarrow 0$, the key expressions turn out to be the same as before. For large values of time, $y(t)$ is again given by (46) and (49) when $r(t)$ is the unit step and unit ramp, respectively. It is also given by (50) and (51) when $d(t)$ is the unit step and unit ramp, respectively.

Although K_D does not influence the steady-state response, it can change the transient behavior significantly. The open-loop transfer function

$$K_c K_p \frac{1 + K_D s}{(s + a)(s + b)}$$

has a zero at $s = -1/K_D$. Root-locus plots for three different zero positions are shown in Figure 14.30. In all three cases, the locus is confined to the left half-plane and the system is always stable. Recall, however, that the distances of the roots from the imaginary axis are the reciprocals of the time constants in the corresponding transient terms. The time constants should be reasonably small so that the transient response dies out quickly. Thus we usually want to move the roots away from the vertical axis. In order to accomplish this, we choose K_D such that the zero at $s = -1/K_D$ is to the left of both open-loop poles, as in part (a) of the figure.

Figure 14.31 shows a typical Bode diagram for the open-loop pole-zero pattern in Figure 14.30(a). The phase margin ϕ_m is always positive, but the gain margin k_m is again undefined because the angle curve does not cross the -180° line.

Proportional-Plus-Integral Control

For a third basic type of controller action, we let

$$G_c(s) = K_c \left(1 + \frac{K_I}{s} \right) = \frac{K_c(s + K_I)}{s} \quad (55)$$

where K_I/s is the transfer function for a component described by $y(t) = K_I \int_0^t x(\lambda) d\lambda$. Inserting (55) into (44) gives

$$\begin{aligned} T_R(s) &= \frac{\frac{K_c K_p (s + K_I)}{s(s + a)(s + b)}}{1 + \frac{K_c K_p (s + K_I)}{s(s + a)(s + b)}} \\ &= \frac{K_c K_p (s + K_I)}{s^3 + (a + b)s^2 + (ab + K_c K_p)s + K_c K_p K_I} \end{aligned} \quad (56)$$

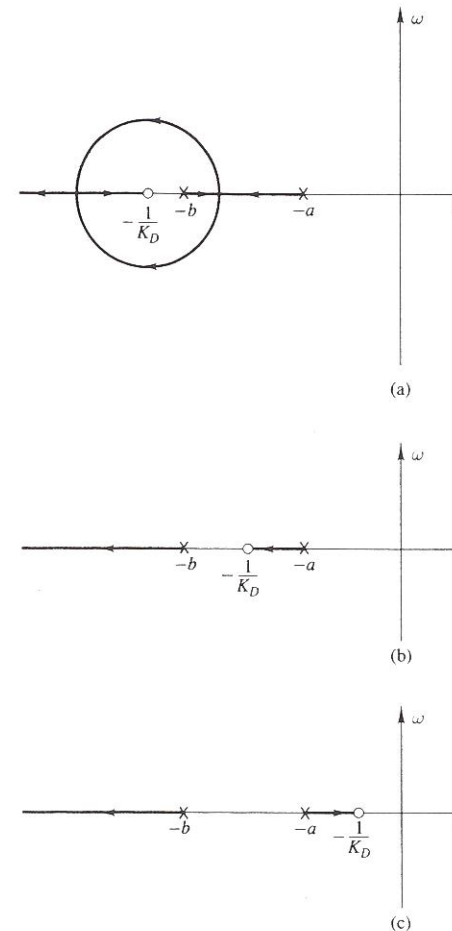
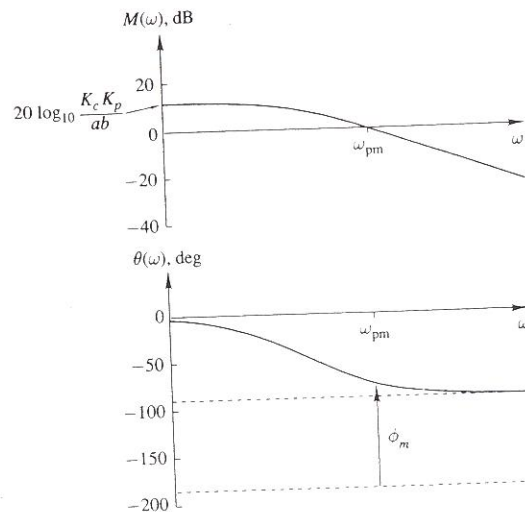


FIGURE 14.30 Possible root-locus plots when $G_c(s) = K_c(1 + K_D s)$.

and

$$\begin{aligned} T_D(s) &= \frac{\frac{K_p}{(s + a)(s + b)}}{1 + \frac{K_c K_p (s + K_I)}{s(s + a)(s + b)}} \\ &= \frac{K_p s}{s^3 + (a + b)s^2 + (ab + K_c K_p)s + K_c K_p K_I} \end{aligned} \quad (57)$$

FIGURE 14.31 Bode diagram when $G_c(s) = K_c(1 + K_D s)$.

We first look at the steady-state response when the disturbance input is zero. When $r(t) = U(t)$, $Y(s) = T_R(s)/s$ and

$$y_{ss} = T_R(0) = \frac{K_c K_p K_l}{K_c K_p K_l} = 1$$

In contrast to the results for the previous types of controllers, the steady-state error is zero for all nonzero values of $K_c K_p K_l$. When $r(t)$ is the unit ramp function,

$$\begin{aligned} Y(s) &= \frac{K_c K_p (s + K_l)}{s^2 [s^3 + (a + b)s^2 + (ab + K_c K_p)s + K_c K_p K_l]} \\ &= \frac{1}{s^2} - \frac{ab/(K_c K_p K_l)}{s} + \dots \end{aligned}$$

and

$$y(t) = t - \frac{ab}{K_c K_p K_l} + \dots$$

The dots represent those terms that decay to zero as t becomes large. Thus the steady-state error to the unit ramp is

$$e_{ss} = \frac{ab}{K_c K_p K_l}$$

Again in contrast to the controllers previously considered, the error for large values of t does not continually increase. In fact, it can be made arbitrarily small by making $K_c K_p K_l$ sufficiently large.

The response to a unit step disturbance input, when $r(t) = 0$, is $Y(s) = T_D(s)/s$. From (57) and the final-value theorem, we see that

$$y_{ss} = 0$$

When $d(t)$ is the unit ramp function, $Y(s) = T_D(s)/s^2$ and

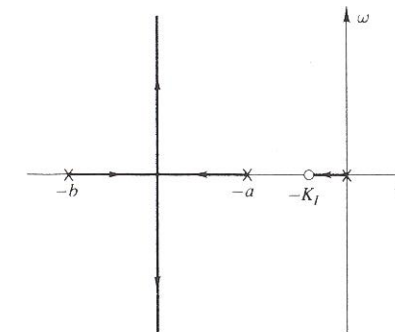
$$y_{ss} = \frac{K_p}{K_c K_p K_l} = \frac{1}{K_c K_l}$$

which becomes small for large values of $K_c K_l$.

For the transient response, we look at the root-locus and Bode diagrams corresponding to the open-loop transfer function

$$\frac{K_c K_p (s + K_l)}{s(s + a)(s + b)}$$

The location of the open-loop zero at $s = -K_l$ is usually chosen close to the pole at the origin, as shown in Figure 14.32. Then the main part of the root-locus diagram will not differ greatly from that for proportional control. There will be another branch of the locus near the origin, and this will result in an additional term in the transient response. Although this term will decay relatively slowly, its magnitude will be small because of the short distance between the pole and the zero of $G_c(s)$.

FIGURE 14.32 Root-locus diagram for $G_c(s) = K_c(1 + K_l/s)$.

The Bode diagram will be similar to the one for proportional control, except at low frequencies. For very small values of ω , the magnitude plot will have a slope of -20 dB per decade, and the angle curve will approach -90° .

Other Types of Control

We have seen that proportional-plus-integral control gives very good steady-state behavior for both reference and disturbance inputs. The dynamic response, however, will be slower than with proportional-plus-derivative response. In order to get both good steady-state and good dynamic characteristics, we can use a controller that combines derivative and integral action. A general proportional-plus-integral-plus-derivative (PID) controller has the transfer function

$$G_c(s) = K_c \left(1 + K_D s + \frac{K_I}{s} \right) \quad (58)$$

Three other basic types of controller characteristics are represented by lead, lag, and lag-lead transfer functions, whose pole-zero patterns are displayed in Figure 14.33. Because some of the poles or zeros may be quite close to the origin and others far away, it can be difficult to indicate their true positions in a single diagram. In the figure, therefore, the diagrams are not to scale but show only the relative pole and zero locations. For comparison, the pole-zero patterns for the PD, PI, and PID controllers are repeated

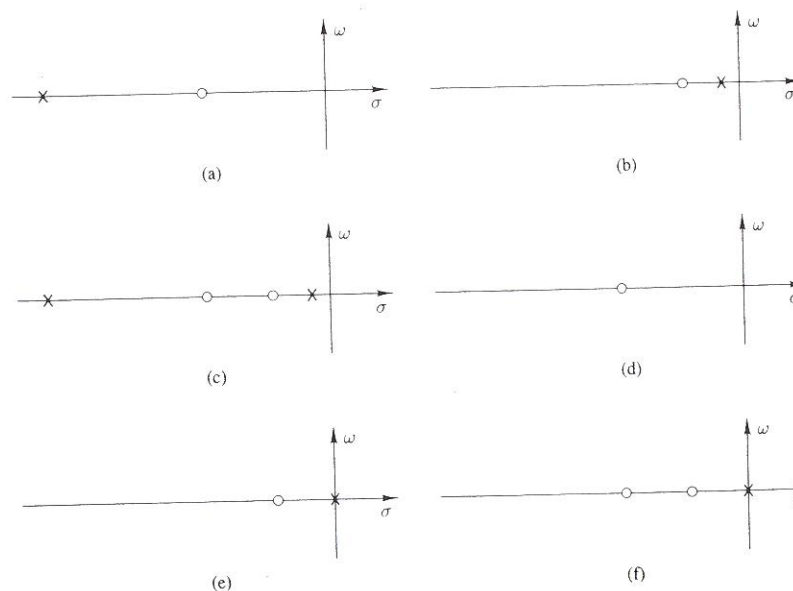


FIGURE 14.33 Relative locations of poles and zeros. (a) Lead compensator. (b) Lag compensator. (c) Lag-lead compensator. (d) PD controller. (e) PI controller. (f) PID controller.

in parts (d), (e), and (f) of the figure. We can see how in some respects they might approximate the lead, lag, and lag-lead transfer functions.

In Figure 14.34, we show Bode plots for typical lead and lag compensators. The Bode diagram for the lag-lead case will be included in the next section. The names for these transfer functions refer to their phase-angle characteristics. Positive and negative values of $\theta(\omega)$ are called leading and lagging angles, respectively. For a lag network, the majority of the changes in the curves normally take place at lower frequencies than for a lead network. Keep in mind that Figures 14.33 and 14.34 show the characteristics only of the controller and not of the entire open-loop transfer function.

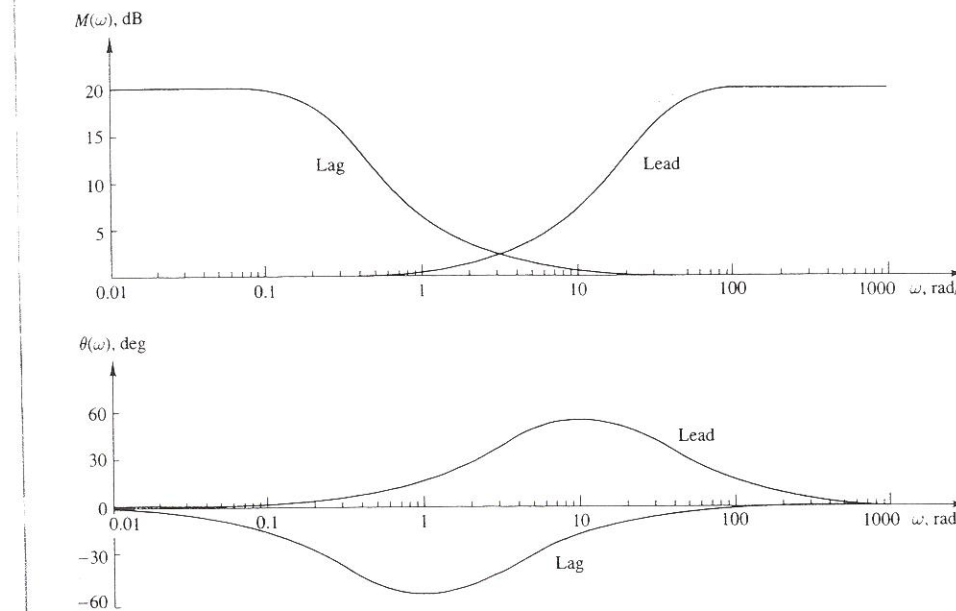


FIGURE 14.34 Bode diagrams for lead and lag compensators.

Many useful transfer functions can be implemented with electrical, mechanical, hydraulic, or pneumatic components. Except for digital controllers, networks employing operational amplifiers are most frequently used. Two of the problems at the end of Chapter 8 presented op-amp networks that can be used for lag, lead, and PID control. Some of the problems at the end of this chapter examine op-amp networks for achieving other types of transfer functions. Because such devices can be incorporated into the controller to compensate for deficiencies that would otherwise exist in the system's behavior, they are often called **compensators**. In some cases, appropriate

compensators are put in the sensor block of Figure 14.25(a) or in an inner feedback loop, rather than in the controller block.

Additional Concerns

A mathematical model provides only an approximate description of the physical system. In the construction of the components, some deviations from the nominal parameter values are to be expected. Wear and environmental factors might further modify their characteristics over time. In any event, not all the secondary features can be incorporated into the model. In fact, there may be some uncertainty in the complete description of the plant to be controlled.

It is important to be sure that the system's behavior will remain acceptable when the parameters undergo moderate changes. It is possible to calculate the effects of individual parameter changes on the responses of the model. Fortunately, the very structure of feedback systems tends to reduce these effects. Even then, however, a safety margin is needed because of uncertainty about how closely the model describes the actual system. Often, factors that may be relatively unimportant under most conditions play a more significant role as the open-loop gain becomes large. Even though the original model might have indicated that the system is always stable, additional poles and zeros may need to be included and may even drive the root locus into the right half-plane for large values of the gain constant K . Nonlinear effects also become increasingly important. More sophisticated models, extensive computer simulation, and testing may be necessary.

The operation of practical sensors and other system components often produces unwanted high-frequency signals in addition to the desired responses. It is important that such internally generated signals, referred to as noise, be attenuated rapidly as they travel around the feedback loop. Thus the decibel curve should fall off sufficiently fast at high frequencies. Associated with the Bode plot there may be specified a cut-off frequency, above which the open-loop gain must be sufficiently small. If the designer is willing to use more costly high-performance components, then this cut-off requirement can be relaxed somewhat.

■ 14.5 APPLICATIONS

We shall illustrate the concepts discussed in Section 14.4 by considering two relatively simple systems. In each case, we shall assume that the system can be represented by Figure 14.25(b) so that $T_R(s)$ and $T_D(s)$ are given by (40). The transfer function of the plant will be specified, will have distinct poles only on the negative real axis, and will have no zeros in the finite s -plane. We assume that we may choose the transfer function $G_c(s)$ for the controller, with no restriction on the values of its coefficients.

In the solutions, we shall assume that there are no constraints other than those given in the problem statements. We shall, however, comment on some of the practical difficulties that one should consider when choosing $G_c(s)$. The design choices that we make will not represent an approach that should always be used, nor will our results be unique. The purpose of this section is simply to introduce some of the important design techniques.

► EXAMPLE 14.17

Let the transfer function of the plant in Figure 14.25(b) be

$$G_p(s) = \frac{10}{(s+1)(s+10)} \quad (59)$$

Assume a unity-feedback system, so that $H(s) = 1$. The steady-state error for a reference step input should not exceed 2% of the input. Similarly, the steady-state response to a disturbance step input should not exceed 2%.

The poles of the closed-loop transfer function $T_R(s)$ should meet the following conditions. The time constants of the corresponding exponential factors in the transient response should be less than 0.1 s. And for any pair of complex conjugate poles, the damping ratio ζ should be at least 0.8.

Determine whether it is possible to satisfy these design constraints by using proportional control. If it is not, use proportional-plus-derivative control to do so.

Solution

The transfer function for the plant is given by (43) with $K_p = 10$, $a = 1$, and $b = 10$. For proportional control, where $G_c(s) = K_c$, we can substitute these numerical values into (45) through (51). From (45), the closed-loop transfer functions for a reference or disturbance input are

$$T_R(s) = \frac{10K_c}{s^2 + 11s + 10(1 + K_c)} \quad (60)$$

$$T_D(s) = \frac{10}{s^2 + 11s + 10(1 + K_c)}$$

When $r(t)$ is the unit step function, the steady-state error is, from (47),

$$e_{ss} = \frac{10}{10 + 10K_c} = \frac{1}{1 + K_c} \quad (61)$$

which should not exceed 0.02. Because we find it generally unwise to choose the controller gain K_c larger than necessary, we let $K_c = 49$.

When $d(t)$ is the unit step function, we see from (50) that the steady-state response is $y_{ss} = 1/(1 + K_c)$. Thus selecting $K_c = 49$ also limits the steady-state response to a constant disturbance input to 2%.

Once K_c has been chosen to meet the steady-state requirements, we have no further means of affecting the dynamic behavior. The denominator

in (60) is the closed-loop characteristic polynomial. Thus with $K_c = 49$, the characteristic equation is

$$s^2 + 11s + 500 = 0 \quad (62)$$

from which the closed-loop poles are at $s = -5.50 \pm j21.67$. The time constant of the exponential factor associated with these poles is $1/5.50 = 0.182$ s. To find the damping ratio, we can compare (62) with $s^2 + 2\zeta\omega_n s + \omega_n^2 = 0$ or we can use (6.52) to write $\zeta = \cos[\tan^{-1}(21.67/5.50)] = 0.246$. The dynamic behavior does not come close to meeting the specifications.

In order to improve the transient response without adversely affecting the steady-state characteristics, we can use a PD controller that has the transfer function

$$G_c(s) = K_c(1 + K_D s)$$

Then the open-loop transfer function becomes

$$G_c(s)G_p(s) = \frac{10K_c(1 + K_D s)}{(s+1)(s+10)} \quad (63)$$

The expressions for $T_R(s)$ and $T_D(s)$ are those in (53) and (54) with $K_p = 10$, $a = 1$, and $b = 10$. As explained in Section 14.4, the parameter K_D has no effect on $T_R(0)$ and $T_D(0)$. Thus we again take $K_c = 49$ in order to satisfy the steady-state specifications.

The extra zero at $s = -1/K_D$ in the open-loop transfer function in (63) should be placed to the left of both the poles, as shown in Figure 14.30(a). Suppose we choose this zero at $s = -15$, plot the root-locus diagram, and then find the point on the locus corresponding to $K_c = 49$. We use MATLAB to do this, with the results shown in Figure 14.35. The pair of closed-loop poles turn out to be at $s = -21.83 \pm j4.83$, corresponding to a time constant $\tau = 0.0458$ s and a damping ratio $\zeta = 0.976$. This is more than satisfactory, so we let $K_D = 1/15 = 0.06667$.

If the dynamic response was not satisfactory, we could reposition the zero at $s = -1/K_D$ and plot a new root-locus diagram. Actually, because the overall transfer function in this example is only second-order, we could achieve the necessary results without plotting an accurate root locus. However, drawing such diagrams is generally a key step in the design of a controller.

► EXAMPLE 14.18

For the plant specified in Example 14.17, we want zero steady-state error when $r(t) = U(t)$ and also zero steady-state response when $d(t) = U(t)$. The conditions on the closed-loop poles are the same as before. The new steady-state requirements could be met with a PI controller, as in (55) through (57). However, the transient response would be no better than that achieved with proportional control. In order to get the improved dynamic

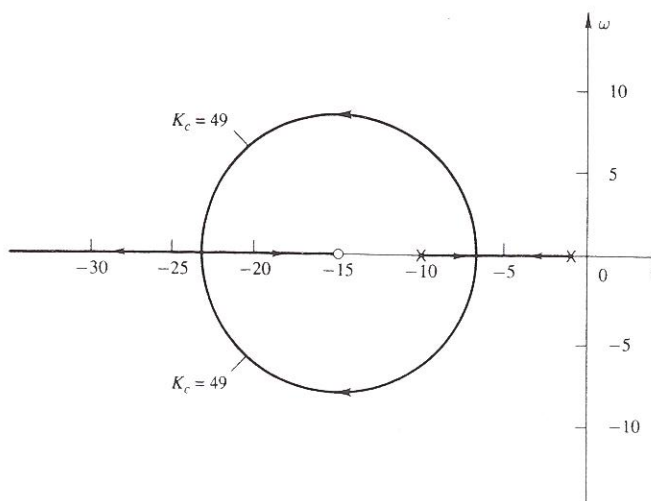


FIGURE 14.35 Root locus for Example 14.17 with PD control.

characteristics associated with derivative action and the excellent steady-state behavior associated with integral action, we use a PID controller that has the transfer function given in (58), which is repeated here.

$$G_c(s) = K_c \left(1 + K_D s + \frac{K_I}{s} \right) = \frac{K_c(K_D s^2 + s + K_I)}{s} \quad (64)$$

Solution

The open-loop transfer function is

$$G_c(s)G_p(s) = \frac{10K_c(K_D s^2 + s + K_I)}{s(s+1)(s+10)} \quad (65)$$

Inserting this expression into (40), with $H(s) = 1$, gives

$$T_R(s) = \frac{10K_c(K_D s^2 + s + K_I)}{s^3 + (11 + 10K_c K_D)s^2 + 10(1 + K_c)s + 10K_c K_I} \quad (66)$$

$$T_D(s) = \frac{10s}{s^3 + (11 + 10K_c K_D)s^2 + 10(1 + K_c)s + 10K_c K_I}$$

Because $T_R(0) = 1$, the steady-state error when $r(t) = U(t)$ is zero for all nonzero values of $K_c K_I$. And because $T_D(0) = 0$, the steady-state response to a constant disturbance input is also zero.

The controller has contributed to the open-loop transfer function in (65) a pole at the origin and two zeros. We shall let one of these zeros be at

$s = -15$, as for the PD controller. The other zero is normally placed close to the pole at the origin, so that the dynamic behavior of the overall system will not be too different from that exhibited when the PD controller is used. We find it convenient to select this zero position at $s = -1$, which is the location of one of the open-loop poles.

Specifying the two zeros of $G_c(s)$ indirectly determines the values of K_D and K_I . For our choice, we find that $K_D = 1/16$ and $K_I = 15/16$. Then (65) can be rewritten as

$$G_c(s)G_p(s) = \frac{(10/16)K_c(s^2 + 16s + 15)}{s(s+1)(s+10)} = \frac{(5/8)K_c(s+1)(s+15)}{s(s+1)(s+10)} \quad (67)$$

We again use MATLAB for this open-loop transfer function to plot the root locus, which is shown in Figure 14.36. Because the steady-state specification is satisfied for all values of K_c , we are now free to select this parameter to place the closed-loop poles anywhere on the locus. The computer program can easily calculate the points on the locus for a given value of K_c and can also determine the value of K_c that corresponds to a specified point. If, for example, $K_c = 20$, the closed-loop poles are at $s = -11.25 \pm j7.81$. The time constant and damping ratio for this pair of poles are $\tau = 1/11.25 = 0.889$ s and $\zeta = \cos[\tan^{-1}(7.81/11.25)] = 0.822$.

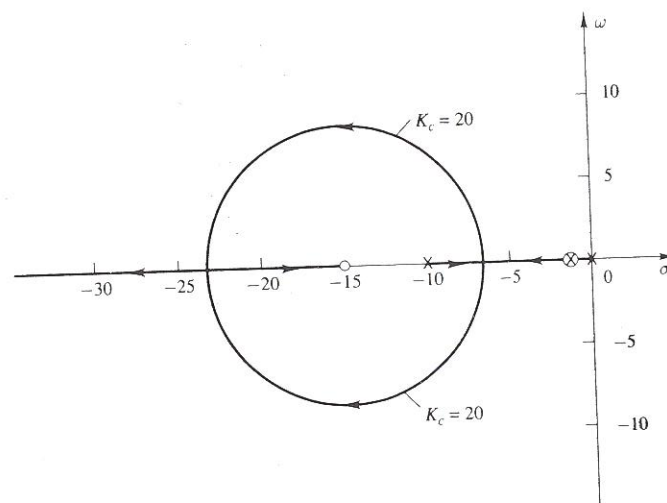


FIGURE 14.36 Root locus for Example 14.18 with PID control.

Although the foregoing choice of K_c satisfies the problem specifications, we should point out two possible problems. First, because of normal toler-

ances in the physical system, the pole and zero at $s = -1$ in $G_c(s)G_p(s)$ cannot be expected to cancel exactly. In addition to modifying the existing branches of the locus somewhat, this creates a third branch, which in turn yields another term in the transient response, with a time constant of about 1 s. However, this transient term is small because of the short distance between the pole and zero.

The second possible problem becomes apparent when we carefully examine the expression for the closed-loop disturbance transfer function. It turns out that, unlike $T_R(s)$, $T_D(s)$ contains a pole at $s = -1$ even if there is an exact cancellation of the pole and zero of $G_c(s)G_p(s)$ at that point. We shall not take the time to investigate the effects of this, but the reader should be aware of it.

Two practical difficulties arise with a PID controller, which was used in the last example. First, it is very difficult with an electronic controller to put a pole of $G_c(s)$ right at the origin of the s -plane. It is more realistic to move this pole slightly to the left of $s = 0$. Second, unwanted noise may be generated within the controller or may appear in the signals leading to it. Because noise contains high-frequency components that should not be amplified, we do not want the magnitude of the controller's frequency-response function $G_c(j\omega)$ to increase at high frequencies.

Consider the Bode diagram shown in Figure 14.37 for the PID controller described by (64), with K_c chosen to be unity and with the values of K_D and K_I that we used in the last example. For very low and very high frequencies, $|G_c(j\omega)|$ becomes K_I/ω and $K_D\omega$, respectively. Thus the low- and high-frequency asymptotes for the magnitude curve have slopes of -20 dB per decade and $+20$ dB per decade, respectively. The low- and high-frequency asymptotes for the angle curve are -90° and $+90^\circ$. The fact that the magnitude approaches infinity as $\omega \rightarrow 0$ and as $\omega \rightarrow \infty$ results in the difficulties described in the previous paragraph. To avoid this, we can use a lag-lead transfer function with the pole-zero pattern shown in part (c) of Figure 14.33.

In order to compare the characteristics of the two controllers, we assume that their multiplying constants have been adjusted so that for both cases, $M(\omega)$ approaches unity in the mid-frequency range. For any controller, increasing the value of K_c just raises the entire magnitude curve by a constant amount without affecting the angle curve. A Bode diagram for the lag-lead controller used in the next example is also shown in Figure 14.37, again for $K_c = 1$. Note that except at low and high frequencies, the two diagrams are quite similar.

► EXAMPLE 14.19

Determine a suitable lag-lead compensator for the plant considered in the last two examples. The steady-state and transient requirements are the same as those given in Example 14.17.

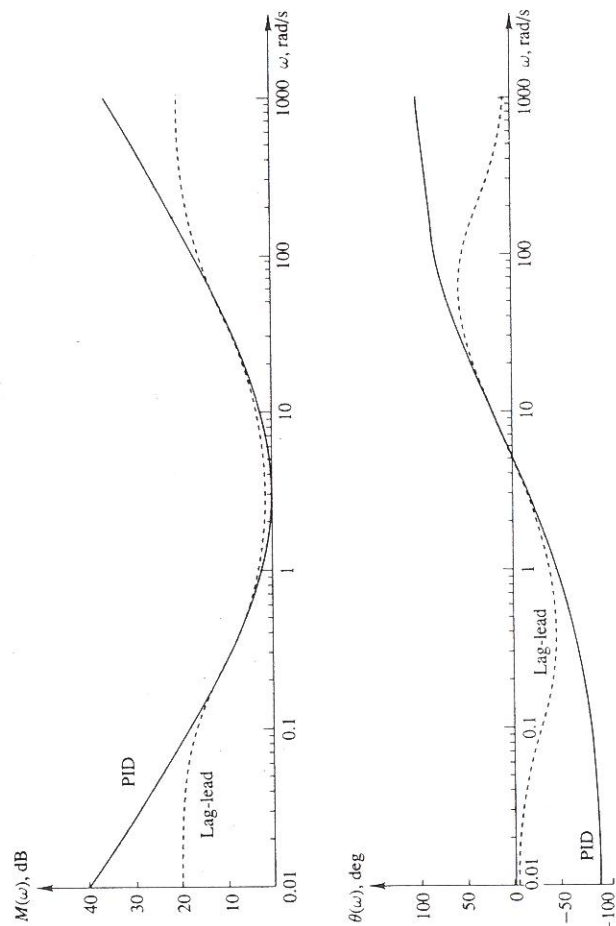


FIGURE 14.37 Bode diagrams for PID and lag-lead controllers.

Solution

The transfer function for the PID controller used in Example 14.18 was

$$\frac{K_c(s+1)(s+15)}{16s}$$

For the lag-lead controller, we keep the same zero positions but move the pole at the origin to $s = -0.1$. We place the new pole at $s = -150$. Then

$$G_c(s) = \frac{10K_c(s+1)(s+15)}{(s+0.1)(s+150)} \quad (68)$$

The multiplying factor of 10 has been added to the numerator so that in the mid-frequency range (say, $3 < \omega < 5$), $M(\omega)$ is approximately the same for the two controllers when the values of K_c are the same. This makes possible a more meaningful comparison of the values of K_c needed for the two cases.

Using (68), we have for the open-loop transfer function

$$G_c(s)G_p(s) = \frac{100K_c(s+1)(s+15)}{(s+0.1)(s+1)(s+10)(s+150)} \quad (69)$$

Substituting this expression into (40), with $H(s) = 1$, gives

$$T_R(s) = \frac{100K_c(s+15)}{s^3 + 160.1s^2 + (1516 + 100K_c)s + (150 + 1500K_c)}$$

$$T_D(s) = \frac{10(s+0.1)(s+150)}{(s+1)[s^3 + 160.1s^2 + (1516 + 100K_c)s + (150 + 1500K_c)]}$$

We see that $T_R(0) = 10K_c/(1 + 10K_c)$. When $r(t) = U(t)$, the steady-state error is

$$e_{ss} = 1 - \frac{10K_c}{1 + 10K_c} = \frac{1}{1 + 10K_c} \quad (70)$$

Because $T_D(0) = 1/(1 + 10K_c)$, the steady-state response when $d(t) = U(t)$ is

$$y_{ss} = \frac{1}{1 + 10K_c} \quad (71)$$

The expressions in (70) and (71) cannot exceed 0.02, so we require $K_c \geq 4.9$.

The root-locus plot for the open-loop transfer function in (69) is shown in Figure 14.38. The values of K_c corresponding to several points of interest are labeled on the diagram. Keep in mind that we may select any value of K_c greater than 4.9. We are not able to show all the branches of the locus,

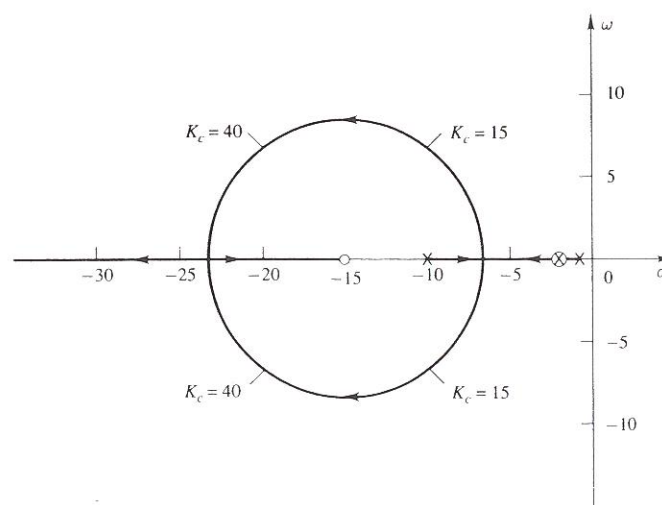


FIGURE 14.38 Root locus for Example 14.19 with lag-lead control.

because the open-loop pole at $s = -150$ is too far to the left. However, the time constant associated with the branch starting at that pole will always be very small.

If a pair of complex closed-loop poles has a real part of -10 , the exponential factor in the corresponding terms in the transient response has a time constant of 0.1 s. This just satisfies one of the conditions on the dynamic behavior. For our locus, it occurs when $K_c = 14.41$. The pair of complex poles are then at $s = -10 \pm j7.443$, which corresponds to a damping ratio $\xi = \cos[\tan^{-1}(7.443/10)] = 0.802$. Because this value is greater than the minimum value allowed by the problem statement, we may choose $K_c = 14.41$. By substituting this value into (70) and (71), we find that in the steady state, the error to a reference step input and the response to a constant disturbance input have both been reduced to 0.69% .

We can improve both the steady-state and the dynamic behavior by making K_c even larger. When $K_c = 40$, for example, the closed-loop poles are at $s = -21.29 \pm j7.65$ and $s = -117.5$. For the pair of complex poles, $\xi = 0.941$ and the time constant is $\tau = 1/21.29 = 0.047$ s. The steady-state error for a constant input, found from (70), is $1/401 = 0.25\%$.

For the plant characteristics given by (59), we can use MATLAB to plot the unit step response for a reference input for different choices of $G_c(s)$. In Figure 14.39, the curves for proportional control and PD control are for

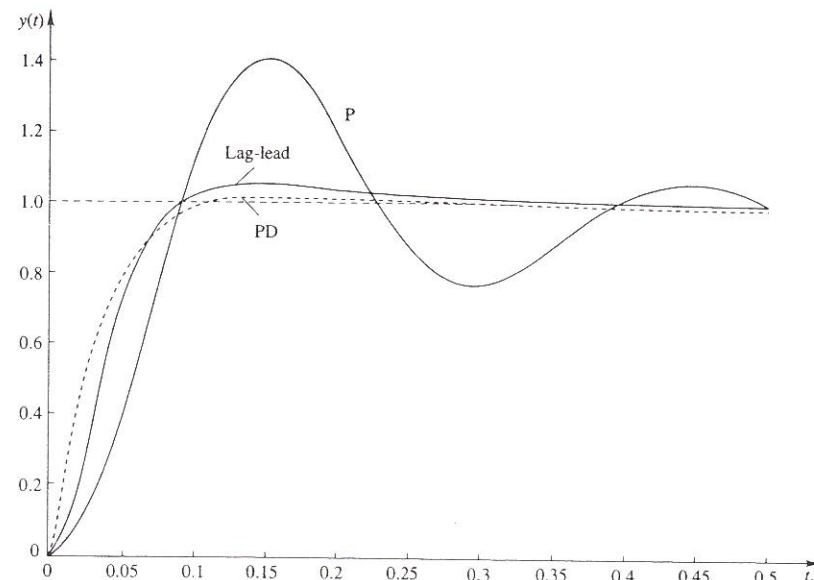


FIGURE 14.39 Unit step responses for a reference input for Examples 14.17 and 14.19.

Example 14.17, both with $K_c = 49$. The curve for lag-lead compensation is for Example 14.19 with $K_c = 40$.

For proportional control, we could have anticipated the large oscillations and the relatively long time to approach the steady state. Recall that the closed-loop poles had a damping ratio $\xi = 0.246$ and a time constant $\tau = 0.182$ s. The curve for proportional-plus-derivative control exhibits excellent dynamic characteristics (corresponding to closed-loop poles with $\xi = 0.976$ and $\tau = 0.046$ s). However, a PD controller would be more sensitive to unwanted noise and in practice would be implemented with a lead compensator.

For the lag-lead design, the pair of dominant complex poles were quite close to those for the PD controller. Because the damping ratio was slightly smaller and the time constant slightly larger, the overshoot and the time to approach the steady state have increased slightly. However, the lag-lead design has a far better steady-state behavior, with an error of only 0.25% instead of 2.0% . Finally, the value of K_c is less than for the other cases.

For any of the designs, a large value of K_c may cause practical difficulties. At some point, the linear model will no longer represent the physical system with reasonable accuracy. As the open-loop gain is increased, unmodeled modes and nonlinearities generally become important. Before selecting a final value of K_c , the designer might run additional computer

simulations using a more complex but more accurate model. In Example 14.19, it may be better to choose $K_c = 15$, which will meet all the specifications given in Example 14.17, than to seek a faster response by using $K_c = 40$.

In the final example, the transfer function $G_p(s)$ for the plant will have three poles and no finite-plane zeros. Increasing the number of poles of $G_p(s)$ without increasing the number of zeros tends to make the system's transient response more difficult to control. Consider the case of a unity-gain feedback system with proportional control. Then the poles and zeros of the feedback system with proportional control are the same as those of $G_p(s)$. From Section 14.2, the number of branches in the root locus that approach infinity is $n - m$, where n and m are the numbers of open-loop poles and zeros, respectively, in the finite s -plane. If $n - m \geq 3$, some of these branches pass into the right half-plane as the gain increases, making the overall system unstable.

Even if a more complicated function were to be used for $G_c(s)$, it would be difficult in practice to add more zeros than poles to the open-loop transfer function. This is because we want to attenuate any high-frequency noise. Nevertheless, we can still choose the poles and zeros of $G_c(s)$ in such a way as to try to pull the root locus to the left in the s -plane.

When the transfer function of the plant has a pole at the origin, the steady-state error for a reference step input is zero. However, there can still be a nonzero steady-state response to a constant disturbance input. In order to illustrate this, let

$$G_p(s) = \frac{K_p}{s(s+a)(s+b)}$$

and $G_c(s) = K_c$. With $H(s) = 1$, we obtain from (40)

$$\begin{aligned} T_R(s) &= \frac{K_c K_p}{s^3 + (a+b)s^2 + abs + K_c K_p} \\ T_D(s) &= \frac{K_p}{s^3 + (a+b)s^2 + abs + K_c K_p} \end{aligned} \quad (72)$$

We see that $T_R(0) = 1$, so there is no steady-state error when $r(t)$ is constant. Because $T_D(0) = 1/K_c$, the steady-state response to $d(t) = U(t)$ is $1/K_c$.

► EXAMPLE 14.20

A particular feedback system can be represented by Figure 14.25(b), with $H(s) = 1$ and with

$$G_p(s) = \frac{500}{s(s+10)(s+50)} \quad (73)$$

The unit step response to $r(t)$ should have a steady-state value of unity, should have an overshoot of less than 15%, and should be within 4% of the steady-state value for all $t > 0.5$ s. The steady-state response to a constant disturbance input should be limited to 1% of the input. Determine a transfer function for the controller that meets these specifications. Because of the practical considerations discussed earlier in this section, the number of finite-plane zeros of $G_c(s)$ should not exceed the number of poles, and none of its poles should be at the origin.

Solution

If $G_c(s) = K_c$, the only poles of the open-loop transfer function will be at $s = 0, -10$, and -50 , which leads to the root-locus plot shown in Figure 14.40. The expressions for $T_R(s)$ and $T_D(s)$ are given by (72) with $K_p = 500$, $a = 10$, and $b = 50$. In order to limit to 1% the steady-state response to a constant disturbance input, we must choose K_c to be at least 100. With $K_c = 100$, the closed-loop poles are at $s = 2.16 \pm j27.80$ and -64.31 , and the system is unstable.

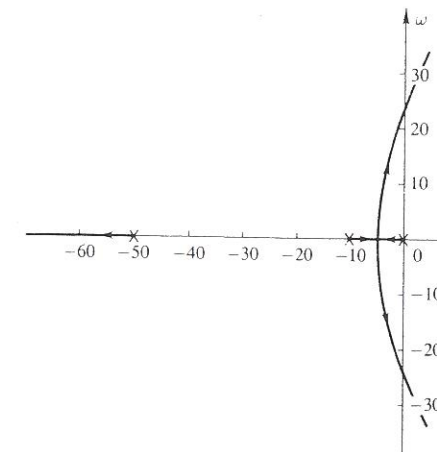


FIGURE 14.40 Root-locus plots for Example 14.20 with $G_c(s) = K_c$.

In order to meet the requirements on both the steady-state and transient behavior, we shall use a lag-lead compensator. We put one zero of $G_c(s)$ at $s = -12$, which is a little to the left of the pole of $G_p(s)$ at -10 , in order to pull to the left the two right-hand branches of the locus. We also put a pole of $G_c(s)$ close to the origin (specifically, at $s = -0.1$) to reduce the steady-state error to a disturbance input.

Associated with the pole at $s = -0.1$ we include a zero at $s = -1$, so that the shape of the root-locus branches moving toward the right half-plane will not be greatly altered. Associated with the zero at $s = -12$ we add a pole at $s = -120$, so that $G_c(s)$ will not have more zeros than poles in the finite s -plane. Once we have selected the zero at $s = -12$ and the pole at $s = -0.1$, it is not uncommon to use a multiplying factor of 10 to locate the additional zero at $-(10)(0.1) = -1$ and the additional pole at $-(10)(12) = -120$. Thus we let

$$G_c(s) = \frac{10K_c(s+1)(s+12)}{(s+0.1)(s+120)}$$

Then the open-loop transfer function becomes

$$G_c(s)G_p(s) = \frac{5000K_c(s+1)(s+12)}{s(s+0.1)(s+10)(s+50)(s+120)} \quad (74)$$

We find that

$$T_R(s) = 5000K_c(s+1)(s+12)/P(s)$$

$$T_D(s) = 500(s+0.1)(s+120)/P(s)$$

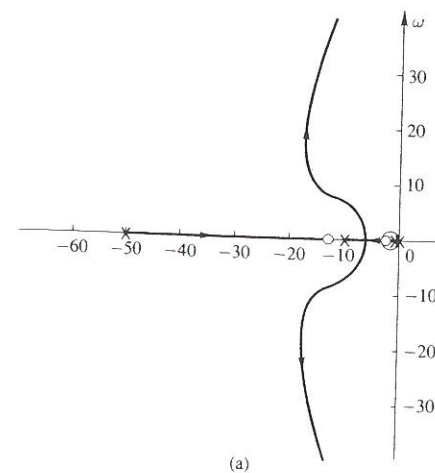
where

$$\begin{aligned} P(s) = & s^5 + 180.1s^4 + 7718s^3 + (60,770 + 5000K_c)s^2 \\ & + (6000 + 52,000K_c)s + 60,000K_c \end{aligned}$$

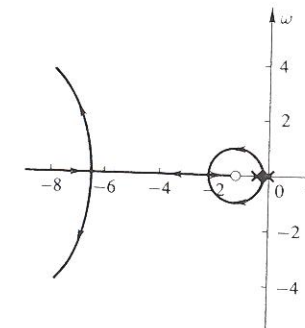
We see that $T_R(0) = 1$ and $T_D(0) = 0.1/K_c$. In order to satisfy the steady-state conditions, we require $K_c \geq 10$.

The root locus for (74) is plotted in Figure 14.41(a). It is difficult to show the entire locus clearly in a single diagram, so the portion near the origin is enlarged in part (b) of the figure. If we choose $K_c = 16$, the closed-loop poles are at $s = -1.96, -19.16, -16.01 \pm j10.63$, and -127.85 . Note that the time constant corresponding to the pole at $s = -1.96$ is $\tau = 1/1.96 = 0.51$ s. However, the magnitude of this term in the transient response will be relatively small because of the presence of the closed-loop zero at $s = -1$.

The response to $r(t) = U(t)$ is shown in Figure 14.42. There is some overshoot because of the complex poles. Because of the pole at $s = -1.96$, the response takes some time to approach its final steady-state value. However, it does satisfy all the conditions in the problem statement.



(a)



(b)

FIGURE 14.41 (a) Root locus for Example 14.20 with lag-lead control. (b) Enlargement of locus near the origin.

We have chosen the examples in this section to illustrate some of the techniques for handling feedback systems and some of the concerns encountered in practice. The availability of computer programs such as MATLAB for quickly plotting root-locus diagrams, Bode diagrams, and time responses is an important asset. An actual design would normally include many more diagrams than we have plotted, showing the effect of varying the controller's characteristics and allowing for the tolerances in physical devices.

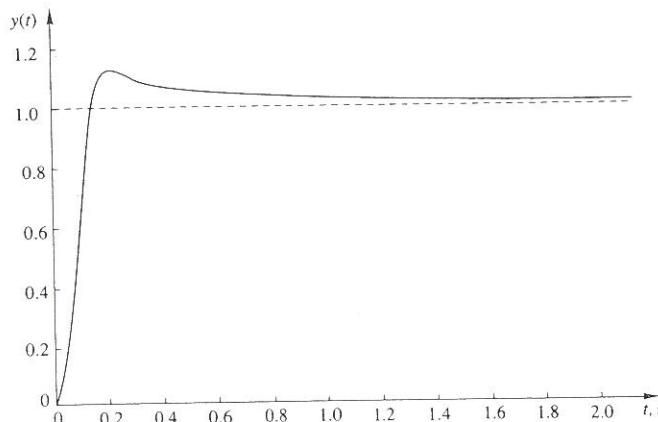


FIGURE 14.42 Unit step response for Example 14.20 with lag-lead control and with $K_c = 16$.

In all our examples, we assumed a simple unity-feedback system, with the compensator placed only in the controller block in the forward path. Had space permitted, we could also have discussed the merits of inserting compensators in the sensor block or in separate inner feedback loops. Note, for example, that the servomechanism examined in Section 14.1 does not exactly fit the configuration assumed in this section.

SUMMARY

Root-locus and Bode diagrams are important tools for analysis and design. Although there are a number of rules to aid a person sketching the diagrams by hand, accurate plots can be obtained easily via standard computer programs. This is especially helpful in an iterative design process, wherein changes in parts of the system are introduced in order to try to improve system performance.

When applied to a feedback system, a root locus shows how the poles of the closed-loop transfer function move in the s -plane as the open-loop gain is increased. Once the locus is drawn, a program such as MATLAB can locate the points corresponding to a particular gain. It can also determine the gain needed to place a closed-loop pole at a particular point on the locus. If the general shape of the locus is not satisfactory, changes can be made in those parameters that are under the designer's control, and a new locus can be plotted.

For any transfer function $T(s)$, we can obtain the frequency-response function by replacing s by $j\omega$ and writing the resulting complex quantity

as $T(j\omega) = M(\omega)e^{j\theta(\omega)}$. To express the magnitude in decibels, we write $M(\omega)|_{dB} = 20 \log_{10} M(\omega)$. In a Bode diagram, we plot $M(\omega)|_{dB}$ versus ω and $\theta(\omega)$ versus ω , using a logarithmic scale for the frequency ω . For a standard feedback configuration, a Bode diagram for the open-loop transfer function can give important information about the behavior of the closed-loop system. An indirect indication of the form of the free response is given by the gain margin and phase margin, which were defined in Figure 14.23. Increasing the open-loop gain raises the magnitude curve by a constant amount without affecting the angle curve.

Among the typical constraints given to the designer of a feedback system are conditions on the steady-state responses to reference and disturbance inputs, as well as conditions on the nature of the transient response. In simple systems, increasing the open-loop gain tends to improve the steady-state response but adversely affects the dynamic behavior. In order to satisfy all the constraints, a more complicated controller may be needed. Root-locus and Bode diagrams help the designer investigate the effects of possible changes in the poles and zeros of the open-loop transfer function.

PROBLEMS

14.1 This problem involves the servomechanism considered in Section 14.1, and the numerical values of the parameters given in Table 14.1 should be used where they are needed.

a) Calculate the value of K_A for a proportional-only controller that will result in a damping ratio of $\zeta = 0.7071$ for the closed-loop system. Give its transfer function $T(s)$ as a ratio of polynomials.

b) Assuming that a tachometer signal $e_3 = K_T \dot{\phi}$ is available for proportional-plus-derivative control, calculate the values of K_A and K_T that will yield a closed-loop system with $\zeta = 0.7071$ and $\omega_n = 8$ rad/s. Determine the closed-loop transfer function and verify that its poles have the specified values for ζ and ω_n .

***14.2** Repeat Problem 14.1 when the desired damping ratio is $\zeta = 1.0$ and, for part (b), the desired undamped natural frequency is $\omega_n = 10$ rad/s.

14.3 Repeat the analysis of Example 14.2 for the series *RLC* circuit with a voltage source that was studied in Example 5.1.

a) Write the transfer function $T(s) = E_R(s)/E_i(s)$, and find its poles in terms of R , L , and C .

b) Assuming that L and C are fixed, find the locus of the poles of $T(s)$ as the resistance R is increased from zero toward infinity. Sketch the locus in the s -plane.

c) Give the value R for which $T(s)$ has a repeated pole ($\zeta = 1$), and give the location of this pole in the s -plane.

14.4 Repeat the analysis of Example 14.2 for the parallel *RLC* circuit with a current source that was studied in Example 5.2.

a) Write the transfer function $T(s) = E_o(s)/I_i(s)$, and find its poles in terms of R , L , and C .

- b) Assuming that L and C are fixed, find the locus of the poles of $T(s)$ as the resistance R is decreased from infinity toward zero. Sketch the locus in the s -plane.
- c) Give the value R for which $T(s)$ has a repeated pole ($\zeta = 1$), and give the location of this pole in the s -plane.
- * 14.5 a) Find the closed-loop transfer function $Y(s)/U(s)$ in terms of the parameter K for the feedback system shown in Figure P14.5.
- b) Write an expression for the closed-loop poles in terms of K , and sketch the locus of these poles in the complex plane for $K \geq 0$. Indicate the pole locations for $K = 0, 1, 2$, and 3 on the locus.

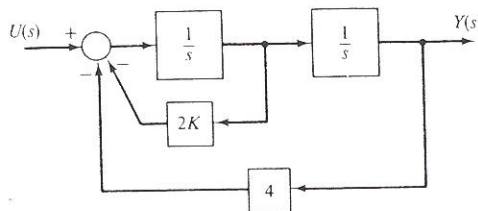


FIGURE P14.5

In Problems 14.6 through 14.14, use the root-locus construction rules presented in Section 14.2 to sketch the root locus for the open-loop transfer function for positive values of the gain K . Also use MATLAB, or another computer package, to obtain a plot of the root locus. Where branches cross the imaginary axis, use the magnitude criterion to find the corresponding value of K , denoted by K^* . Identify the open-loop zeros and poles with the symbols \circ and \times , respectively, and use arrows to show the directions in which the roots move for increasing gain. Give the value for σ_0 , the center of the large-gain asymptotes, where it exists.

$$14.6 G(s)H(s) = \frac{K}{s(s+4)(s+6)}$$

$$14.7 G(s)H(s) = \frac{K}{(s+2)(s+5-j3)(s+5+j3)}$$

$$14.8 G(s)H(s) = \frac{K(s+2)}{(s+1)(s+3)(s+6)}$$

$$* 14.9 G(s)H(s) = \frac{K(s+9)}{(s+1)(s+2)(s+4)(s+8)}$$

$$14.10 G(s)H(s) = \frac{K(s^2+12s+37)}{s^2+4s+29}$$

$$14.11 G(s)H(s) = \frac{K(s+4)}{(s+1)(s-1)}$$

$$14.12 G(s)H(s) = \frac{K(s+2)}{(s+1)^2(s+8)}$$

$$14.13 G(s)H(s) = \frac{K(s+6)}{(s+1)(s+4)^2}$$

$$* 14.14 G(s)H(s) = \frac{K}{(s+1)(s+3)(s+6)(s+12)}$$

14.15 Repeat Example 14.5 when $K < 0$.

* 14.16 Repeat Problem 14.9 when $K < 0$.

In Problems 14.17 through 14.21, sketch Bode plots for the frequency-response functions specified. In each case, include a magnitude curve in decibels and a phase-angle curve in degrees. Use a logarithmic frequency axis for both curves. Also use MATLAB, or another analysis package, to obtain a computer-generated Bode plot.

$$14.17 T(j\omega) = \frac{1+j\omega/2}{1+j\omega/50}$$

$$14.18 T(j\omega) = \frac{1+j\omega/5}{(1+j\omega/40)^2}$$

$$14.19 T(j\omega) = \frac{1+j\omega/20}{(1+j\omega/2)(1+j\omega/50)}$$

$$14.20 T(j\omega) = \frac{1}{j\omega(1+j\omega/50)}$$

$$14.21 T(j\omega) = \frac{j\omega}{1+j\omega/40}$$

14.22 Construct the Bode diagram for the transfer function

$$T(s) = \frac{\omega_n(s + \omega_n)}{s^2 + 2\zeta\omega_n s + \omega_n^2}$$

when the damping ratio is $\zeta = 1, 0.5$, and 0.1 . Use the normalized frequency ω/ω_n for the abscissa. Compare the curves with those for Example 14.15, giving special attention to the low- and high-frequency asymptotes and to the point at $\omega/\omega_n = 1$.

14.23 a) Obtain a computer-generated Bode diagram for the open-loop transfer function in Example 14.5, with $K = 100$. Determine the gain margin and the phase margin.

b) Find the value of K that will give a gain margin of 10 dB.

c) Find K^* , the maximum value of K for which the closed-loop transfer function will be stable.

* 14.24 Repeat Problem 14.23 for the open-loop transfer function in Example 14.7, with $K = 40$.

14.25 a) Use the result of Example 8.16 to verify that the transfer function for the circuit shown in Figure P14.25 is

$$\frac{E_o(s)}{E_i(s)} = -\frac{R_3(R_4C_4s + 1)[(R_1 + R_2)C_2s + 1]}{R_1(R_2C_2s + 1)[(R_3 + R_4)C_4s + 1]}$$

b) Express the poles and zeros in terms of the resistances and capacitances. Plot the pole-zero pattern, assuming that $R_4C_4 > (R_1 + R_2)C_2$.

c) By referring to Figure 14.33, identify the type of controller or compensator that the circuit implements.

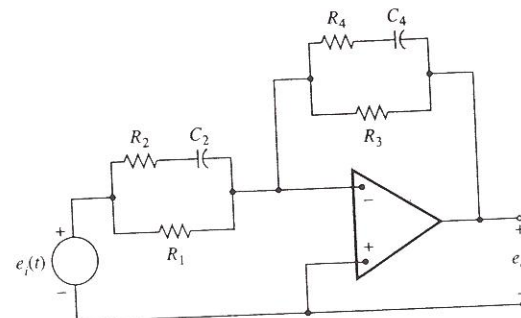


FIGURE P14.25

- * 14.26 a) Use the result of Example 8.16 to determine the transfer function $E_o(s)/E_i(s)$ for the circuit shown in Figure P14.26.
 b) Express the poles and zeros in terms of R_1 , R_2 , and C . Plot the pole-zero pattern.
 c) By referring to Figure 14.33, identify the type of controller or compensator that the circuit implements.

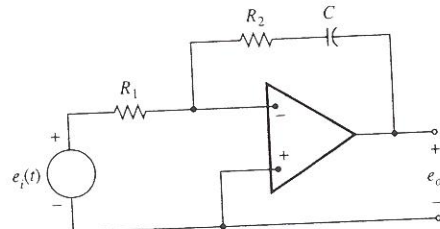


FIGURE P14.26

- 14.27 Repeat Problem 14.26 for the circuit shown in Figure P14.27.

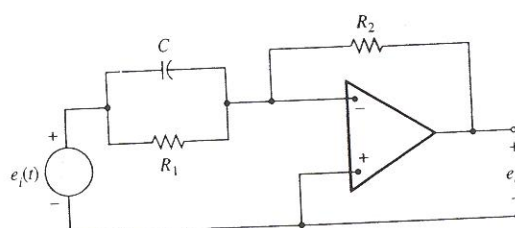
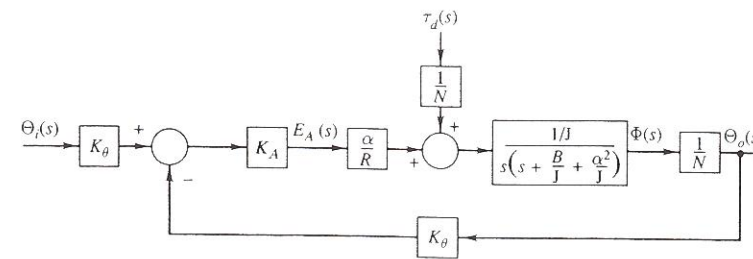


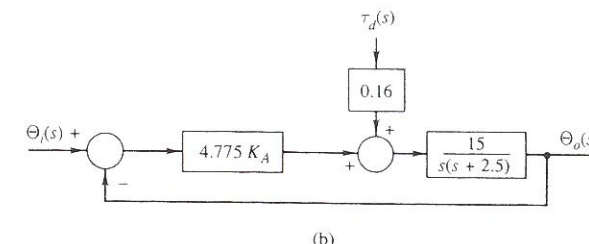
FIGURE P14.27

- * 14.28 The servomechanism discussed in Section 14.1 has a disturbance torque $\tau_d(t)$ applied to the shaft to which the output potentiometer is attached. In Figure 14.1, the positive sense of this torque is clockwise.

- a) Show that the block diagram of Figure 14.2 must be modified to appear as in Figure P14.28(a).



(a)



(b)

FIGURE P14.28

- b) When $R = 8 \Omega$, $\alpha = 5.0 \text{ V} \cdot \text{s}/\text{rad}$, and the two potentiometer gain blocks K_θ are moved to the output of the summing junction and combined with the amplifier gain block K_A , verify that the model can be represented as shown in Figure P14.28(b). Use the numerical values in Table 14.1.

- c) Assume that proportional control is used with $K_A = 0.08727 \text{ V/V}$. Determine the steady-state errors to

- A unit ramp input in the reference angle $\theta_r(t)$.
- A unit step in the disturbance torque $\tau_d(t)$.

- d) Draw a root-locus plot and determine the value of K_A that will result in a closed-loop system having $\zeta = 0.8$. Find the corresponding value of ω_n .

- e) Draw a Bode plot for the open-loop system when $K_A = 0.4$ and determine the phase margin. Explain why the gain margin is not defined.

- 14.29 The servomechanism discussed in Section 14.1 is to be controlled by inserting a proportional-plus-derivative (PD) compensator immediately after the amplifier.

- a) Verify that the system can be represented by the block diagram shown in Figure P14.29, where K_D is the derivative gain, in seconds.

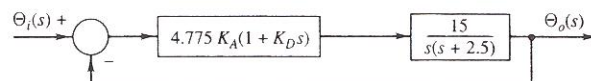


FIGURE P14.29

- b) Show analytically that when the derivative gain is $K_D = 0.1 \text{ s}$, it is possible to have closed-loop poles with $\zeta = 0.5$ and $\omega_n = 5.0 \text{ rad/s}$. Determine the required value of the amplifier gain K_A .
- c) Draw a root-locus plot and verify the locations of the closed-loop poles for the value of K_A found in part (b).
- d) Using MATLAB or another computer program, compute and plot the response of the closed-loop system to a unit step in the reference input $\theta_r(t)$.
- 14.30** The servomechanism discussed in Section 14.1 is to be controlled by inserting a lead compensator immediately after the amplifier.

a) Verify that when the magnitude of the lead pole is 10 times that of the lead zero, the system can be represented by the block diagram shown in Figure P14.30.

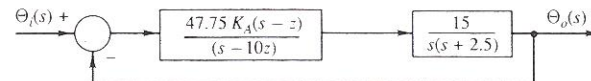


FIGURE P14.30

- b) Draw the root-locus plot with the lead zero placed at $s = -10$, and show that the upper branch of the locus passes close to the point in the s -plane that corresponds to $\zeta = 0.5$ and $\omega_n = 5.0 \text{ rad/s}$. Select a value for the amplifier gain K_A that will result in closed-loop poles close to this point, and determine the locations of all the closed-loop poles for this value of K_A .
- c) Using MATLAB or another computer program, compute and plot the response of the closed-loop system to a unit step in the reference input $\theta_r(t)$.
- 14.31** The servomechanism discussed in Section 14.1 has a disturbance torque $\tau_d(t)$ as described in Problem 14.28 and is to be controlled with a lag-lead compensator.

a) Adapt the block diagram in Figure P14.28(b) to have the controller transfer function

$$G_c(s) = \frac{10K_A(s+1)(s+10)}{(s+0.1)(s+100)}$$

in place of the gain K_A .

- b) Evaluate the closed-loop transfer functions from each of the inputs to the output.
- c) Solve for the steady-state error in θ_o that is due to a unit step in the disturbance torque $\tau_d(t)$.
- d) Draw the root-locus plot and determine the value of K_A that will result in closed-loop poles with $\zeta = 0.7$. Determine the locations of all the closed-loop poles for this value of K_A .

- e) Using MATLAB or another computer program, compute and plot the response of the closed-loop system to a unit step in the reference input $\theta_r(t)$.
- * **14.32** Figure P14.32 shows a thermal process with a feedback temperature controller. The controller receives the desired temperature $\theta_d(t)$ and the measured temperature θ_m as inputs and determines the heat q_h supplied by the heater. The uncontrolled process was modeled in Example 11.7, where we derived transfer functions for $\hat{\Theta}(s)/\hat{Q}_h(s)$ and $\hat{\Theta}(s)/\hat{\Theta}_i(s)$. Assume that the thermal resistance R is infinite and that the liquid flow rate is \bar{w} , a constant. In terms of incremental variables, the controller is modeled by the relationship

$$\hat{Q}_h(s) = G_c(s)[\hat{\Theta}_d(s) - \hat{\Theta}_m(s)]$$

where $G_c(s)$ is the controller transfer function and the quantity $\hat{\Theta}_d(s) - \hat{\Theta}_m(s)$ is the transform of the measured temperature error. It is assumed that the sensor measures the actual temperature exactly—that is, $\hat{\theta}_m = \hat{\theta}$.

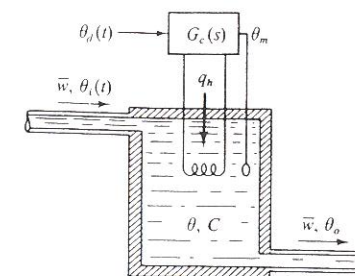


FIGURE P14.32

- a) Draw a block diagram representing the closed-loop system that has the incremental inputs $\hat{\Theta}_d(s)$ and $\hat{\Theta}_i(s)$ and the incremental output $\hat{\Theta}(s)$.
- b) Evaluate the closed-loop transfer functions $\hat{\Theta}(s)/\hat{\Theta}_d(s)$ and $\hat{\Theta}(s)/\hat{\Theta}_i(s)$ in terms of the unspecified controller transfer function $G_c(s)$.
- c) Using proportional control with $G_c(s) = K_c$, evaluate the two closed-loop transfer functions $\hat{\Theta}(s)/\hat{\Theta}_d(s)$ and $\hat{\Theta}(s)/\hat{\Theta}_i(s)$. Show that for step inputs in $\hat{\theta}_d(t)$ and $\hat{\theta}_i(t)$, taken separately, the steady-state temperature error is not zero for finite values of K_c .
- d) Using proportional-plus-integral control with $G_c(s) = K_c(1 + K_I/s)$, reevaluate the closed-loop transfer functions. Show that for step inputs in $\hat{\theta}_d(t)$ and $\hat{\theta}_i(t)$, taken separately, the steady-state temperature error is zero for all positive values of K_c and K_I .

- 14.33** Repeat the analysis of the temperature-control system described in Problem 14.32 when a dynamic model for the temperature sensor is included. Ignore possible fluctuations in the inlet temperature so that $\hat{\theta}_i(t)$ can be taken to be zero. In terms of the incremental variables, the sensor is assumed to have the transfer

function

$$\frac{\hat{\Theta}_m(s)}{\hat{\Theta}(s)} = \frac{1}{as + 1}$$

where a is the sensor time constant.

- a) Find the closed-loop transfer function $\hat{\Theta}(s)/\hat{\Theta}_d(s)$ for proportional control, where $G_c(s) = K_c$. Determine the steady-state error to a step input in $\hat{\theta}_d(t)$.
- b) Repeat part (a) for PI control, where $G_c(s) = K_c(1 + K_I/s)$.

14.34 Figure P14.34 shows a liquid-level control system such as might be found in a typical chemical process. The sensed level signal h_s is obtained by measuring the gauge pressure p_1^* at the bottom of the tank. The controller also receives a signal $h_d(t)$ indicating the desired level. The controller output x is used to position a linear control valve in a bypass line connected around a centrifugal pump. The bypass flow rate w_b is given by

$$w_b = k\sqrt{\Delta p} \left(\frac{x}{x_m} \right)$$

where x_m is the maximum valve opening, x is the actual valve opening, Δp is the pressure difference developed by the pump, and k is the valve coefficient. The pump is driven at a constant speed, and at the operating point, the slope of the curve of Δp versus w is $-K$.

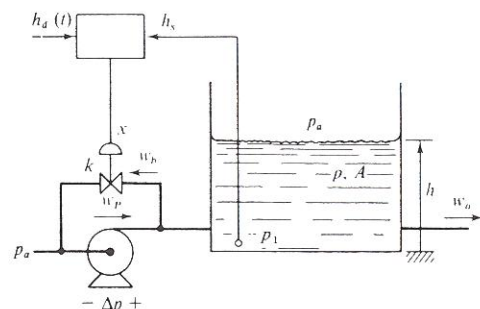


FIGURE P14.34

- a) Derive the linearized model of the control valve by finding the coefficients α and β in the expression $\hat{w}_b = \alpha \hat{\Delta p} + \beta \hat{x}$.
- b) Write the linearized system equations in terms of the incremental variables \hat{h} , \hat{w}_o , \hat{w}_b , \hat{w}_p , $\hat{\Delta p}$, and \hat{p}_1 . Then draw the block diagram of the open-loop system with $\hat{X}(s)$ and $\hat{W}_o(s)$ as the inputs and $\hat{H}(s)$ as the output. Evaluate the transfer functions $\hat{H}(s)/\hat{X}(s)$ and $\hat{H}(s)/\hat{W}_o(s)$.

c) Taking $\hat{W}_o(s) = 0$, draw a block diagram of the closed-loop system when the controller is described by $\hat{X}(s) = K_c[\hat{H}_d(s) - \hat{H}_s(s)]$ and the sensor is described by $\hat{H}_s(s) = \hat{H}(s)$. Find the closed-loop transfer function $\hat{H}(s)/\hat{H}_d(s)$. Explain why the controller gain K_c should be negative.

d) Repeat part (c), using a dynamic model of the sensor such that $\hat{H}_s(s)/\hat{H}(s) = 1/(\tau s + 1)$.